# Canadian Contractor Report of Hydrography and Ocean Sciences 56

## 2011

## GPR Capabilities for Ice Thickness Sampling of Low Salinity Ice and for Detecting Oil-In-Ice

by

**Louis Lalumiere**

**Sensors by Design Ltd.,**
**100 Peevers Crescent,**
**Newmarket, Ontario, L3Y 7T1**

# Table of Contents

## ABSTRACT

L. Lalumiere, 2011. GPR Capabilities for Ice Thickness Sampling of Low Salinity Ice and for Detecting Oil-In-Ice.   Can. Contract. Rep. Hydrogr. Ocean Sci. 56: iv+ 36pp.

The BIO helicopter sensor system developed for Dr. Simon Prinsenberg of the Bedford Institute of Oceanography (BIO) includes a number of helicopter-borne sensors for monitoring snow and ice conditions. During recent field surveys a ground-penetrating radar system (GPR) has been used over brackish water of Lake Melville (Labrador) and a tidal river in Prince Edward Island (P.E.I.) to test the capabilities of the GPR to monitor snow and ice properties. Tests of the performance of a Noggin 1000 GPR and Noggin 500 GPR to measure the thickness of brackish ice have been made and will be discussed in this report.
Another application for the airborne GPR being explored was its capability to detect of oil in or below sea ice. This report documents other researchers work in this area and compares the measurement technique these researchers have proposed with the GPR processing technique used for snow and freshwater ice thickness. Also, the author gives his opinion on the likelihood of the success of GPR as an oil-in-ice detector.

# Résumé

Lalumiere, L., 2011. *GPR Capabilities for Ice Thickness Sampling of Low Salinity Ice and for Detecting Oil-In-Ice.*   Can. Contrat. Rep. Hydrogr. Ocean Sci. 56: iv+ 36 pages.

Le système de détection de l'hélicoptère de l'IOB, conçu pour M. Simon Prinsenberg (Ph. D.) de l'Institut océanographique de Bedford (IOB), comporte un certain nombre de capteurs héliportés servant à surveiller les conditions de neige et de glace. Au cours de récents relevés sur le terrain, on a utilisé un géoradar pour évaluer la capacité du système à déterminer les propriétés de la neige et de la glace des eaux saumâtres du lac Melville (Labrador) et d'une rivière à marées de l'Île-du-Prince-Édouard. Des essais de performance ont été effectués pour vérifier la capacité des géoradars Noggin 1000 et Noggin 500 à mesurer l'épaisseur de la glace saumâtre; les résultats de ces essais seront présentés dans le présent rapport.
Un autre aspect du géoradar aéroporté qui a été évalué est sa capacité à détecter la présence de pétrole dans ou sous la glace marine. Le présent rapport contient l'examen des travaux d'autres chercheurs du domaine et une comparaison des techniques de mesure proposées par ces chercheurs en lien avec la technique de traitement du géoradar utilisée pour mesurer l'épaisseur de la neige et de la glace d'eau douce. De plus, l'auteur nous fait part de son point de vue sur le succès probable du géoradar à titre de détecteur de pétrole dans de la glace.

# 1  INTRODUCTION

## 1.1  SCOPE

The BIO helicopter sensor system developed for Dr. Simon Prinsenberg of the Bedford Institute of Oceanography (BIO) includes a number of helicopter-borne sensors for monitoring snow and ice conditions. Recent survey work has included the testing of an off-the-shelf ground-penetrating radar system (GPR) to provide snow and freshwater ice thickness reported in [2] and [3]. This report documents the use of the GPR over low salinity ice that was encountered in Lake Melville (Labrador) and a tidal river in Prince Edward Island (P.E.I.).  Additionally, this report details the usage of the GPR component of the BIO helicopter-borne sensor suite for possible use for the detection of oil-in-ice in the event of an oil spill in the Arctic ice.

## 1.2  EQUIPMENT USED

The GPR system used is a Noggin NIC 1000 from Sensors and Software Inc. of Mississauga, Ontario. A photograph of the Noggin 1000 antenna unit and NIC controller is shown is Figure 1.1. The Noggin 1000 is 30cm long by 15cm wide and 12cm high. For the 2009 Labrador field work, the Noggin 1000 was mounted in a boom mounted under a Bell 206L helicopter. For the 2010 P.E.I. field work, the Noggin 1000 was mounted in a pod which was attached to the skid gear of a B0105 helicopter. For the 2010 P.E.I. field work, a Noggin 500 GPR unit was rented from Sensors and Software.  The Noggin 500 is 39cm long by 22cm wide and 16cm high and can be mounted inside a BO105 skid-gear pod. Though it provides lower resolution than the Noggin 1000, the Noggin 500 has better system performance to penetrate through brackish ice than the Noggin 1000.



Figure 1.1 Sensors and Software Noggin 1000 GPR and NIC control unit (left) and the mounting boom under the Bell 206L Helicopter (right).

The Noggin was configured to collect GPR scans composed of 500 samples with a sampling interval of 0.1 ns providing an echo return window of 50ns starting at 20ns after the transmitter fires. With

these settings, the helicopter flying height range must be maintained between 3m and 10.5m in order for the surface echo to be seen in the GPR data. The vertical axes of the plots shown in this report are scaled to show the helicopter flying height over the first echo returned and used a constant radar velocity in air. To compensate for the varying radar velocities in air, snow and ice, this scale needs to be reduced by a factor of 0.8 for GPR echoes from the snow-to-ice interface and by a factor of 2 for GPR echoes from the ice-to-water interface. This is done in post processing plots but not in the near-real time display software to check on data quality while surveying. With a scan rate of 30 scans per second and a typical flying speed of 60 knots, the ground spacing is approximately 1m between scans.

## 1.3   DATASETS USED

### 1.3.1   APRIL 2009 LAKE MELVILLE DATASET

Helicopter-born GPR data were collected from the ice of Lake Melville in April 2009. Lake Melville is located in the Canadian province of Newfoundland and Labrador. The Lake is a fjord that is connected to the Labrador Shelf and has a saline bottom layer overlain with a seasonal varying low saline layer during the open-water season or freshwater layer during the ice-covered season due to river runoff. The vertical salinity and resulting density structure varies along the long (E-W) axis of the Lake as the freshwater due to runoff moves out of the fjord to the Labrador Shelf. As the ice grows on the lake, it is formed from water of varying salinity and thus Lake Melville provides an excellent area to determine the capability of the GPR to penetrate through the ice for varying ice salinities. Figure 1.2 shows the survey areas on Lake Melville. To provide a scale for the plot, the white line shows the track for GPR line 583 that is approximately 25 km long.



Figure 1.2 - Google Earth image locating the GPR profiles flown over Lake Melville

## 1.3.2 FEBRUARY 2010 PEI DATASET

This data set has GPR profiles collected with the Noggin 1000 and the Noggin 500. GPR lines were flown over a small freshwater lake using both the Noggin 1000 and the Noggin 500. These lines are shown on a Google Earth plot in Figure 1.3. The Noggin 500 was used for the GPR lines flown over the Hillsborough River. These lines are shown on a Google Earth plot in Figure 1.4.



Figure 1.3 - Google Earth image locating the Noggin 500 and Noggin 1000 GPR profiles flown over a small Lake in Prince Edward Island.



Figure 1.4 - Google Earth image locating the Noggin 500 GPR profiles flown over the Hillsborough River in Prince Edward Island.

# 2 LOW SALINITY ICE THICKNESS MEASUREMENTS

This section covers the following topics:
- Two-layer GPR snow and ice thickness measurement technique
- GPR plots over ice with changing salinity
- Comparison of Noggin 500 with Noggin 1000

The plots in this section were collected on Saturday March 21, 2009 over ice cover of Lake Melville. The GPR plots are sequenced to present each plot moving easterly (seaward) down Lake Melville - though they were collected in the reverse order. The first plot is GPR line 584 where the ice was made up from fresh water. The GPR profile 583 is a 25 km long plot with fresh water beneath the ice cover on the west end and brackish water on the east end; based on an interpretation of the GPR data. Also shown are GPR plots flown over three stations in the eastern half of Lake Melville. E-W and S-N GPR lines were flown at each site, centered at locations where on-ice station data was collected (Table 1, shown later). Figure 1.2 plots the GPS tracks for these profiles on a Google Earth image.

Appendix A has additional discussion and example plots showing enhanced signal processing used to view weak GPR echoes from profiles collected over the brackish ice.

## 2.1 TWO-LAYER GPR SNOW AND ICE THICKNESS MEASUREMENT TECHNIQUE

Previous publications [1] and [2] have described the snow thickness processing algorithm that has been used for measuring snow thicknesses over sea ice. As sea ice is very conductive, there is typically no GPR echo returned from the ice-to-water interface. This permits a simple algorithm to be used to detect the air to snow interface echo and the snow to ice interface echo and use the time difference of arrival of the two echoes to measure snow thickness.

The snow thickness over sea ice processing software does not work when over low saline ice as the ice-water GPR echo also exists and confuses the software algorithm. Thus a new three step processing routine was created to measure both the snow and the ice layer thicknesses. The algorithm does the following:
- Top of snow - find the first echo in the scan
- Top of ice - find the largest echo in a predetermined region arriving later than the top of snow echo
- Bottom of ice - find the largest echo in a predetermined region arriving later than the top of ice echo

Prior to locating the echo peaks, the GPR data is smoothed using the Matlab Filtfilt function to apply a 3 scan running average along the profile. The top layer has a median filter applied to clean up large outliers. The search for the echo position of the lower layers begins at an offset from the upper layer.

## 2.1.1 PLOT OF GPR DATA TAKEN OVER SNOW AND FRESHWATER ICE

GPR data from a Lake Melville profile collected on March 21, 2009 were processed to extract snow and ice thicknesses. Figure 1.2 shows a Google Earth screen capture showing the flight track of the two GPR profiles. The Lake Melville profile is approximately 6.7km long for 1.11 metres per scan.

GPR line number 584 is from the south west end of the lake and the ice salinity is near zero according to the survey's field notes [3].

Figure 2.1 shows a GPR profile plot for line D2009_080F584 (referred to as line 584) over Lake Melville. This plot consists of a 1 km section taken near the end of the complete GPR profile (from scan numbers 4270 to 5320) which is at the westerly end of the profile track shown in Figure 1.2. On the right hand side, the GPR echo from the bottom of the ice is very consistent. On the left, the ice echo is intermittent.
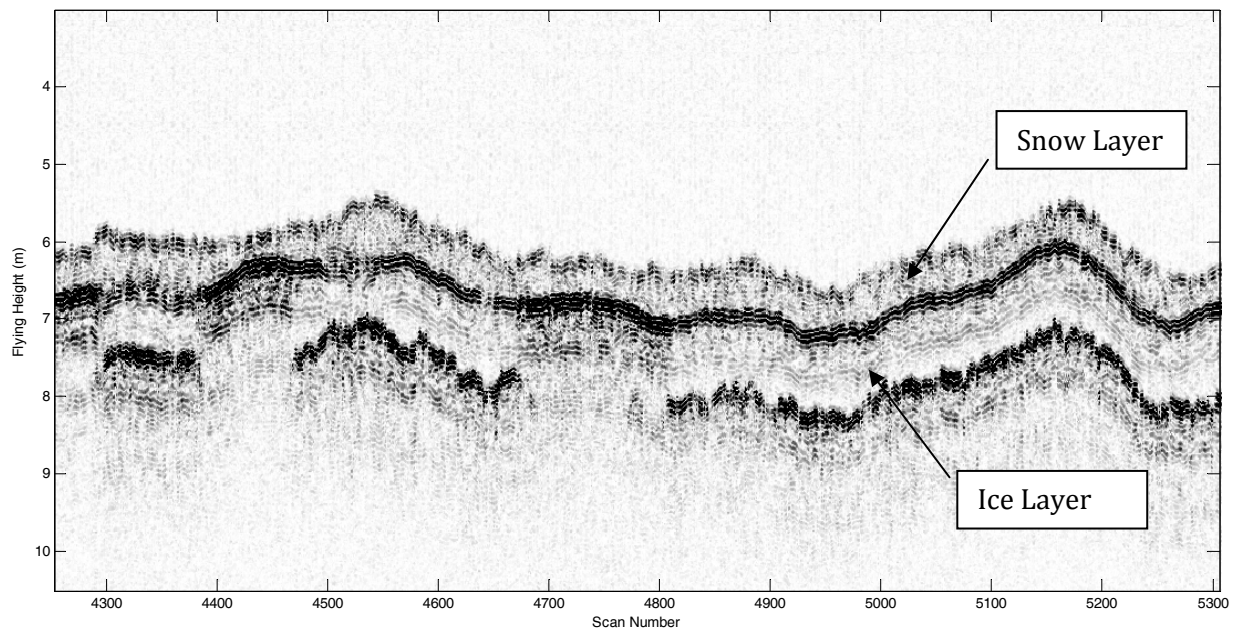


Figure 2.1 - A GPR profile plot over Lake Melville from the end of line 584. The annotations show the snow layer and the ice layer. This plot consists of a 1 km section taken near the end of the complete GPR profile.

Figure 2.2 shows a complete profile plot for line 584, annotated to show the detected top of snow, top of ice and bottom of ice layers as determined from the two-layer snow and ice thickness processing. The ice layer is visible for most of the profile.
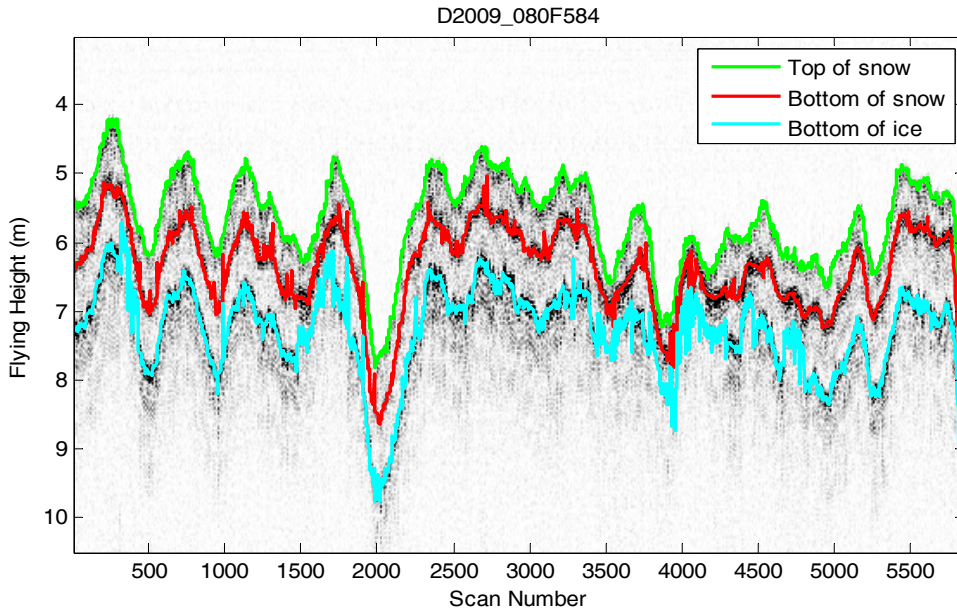
Figure 2.2 - Lake Melville F584 GPR profile plot (6.7km length) with the detected layers plotted.

Figure 2.3 shows snow thickness and ice thickness plots using the detected layer positions. The profile shows snow thickness approximately 60 cm thick and ice approximately 50 cm thick on Lake Melville. The ice thickness processing appears to track the ringing in the ice in the areas where the brackish ice appears; i.e. in the vicinity of scan 400, between scans 1500 and 1800 and from scan 3400 to 4800. This phenomenon of thin brackish ice with a thinner layer of snow in between thicker ice and larger snow depths is not well understood and needs to be verified with additional data collection, and possibly variable surface layer currents and vertical mixing increased due to bottom topographic effects on the evolution of the pack ice growth.
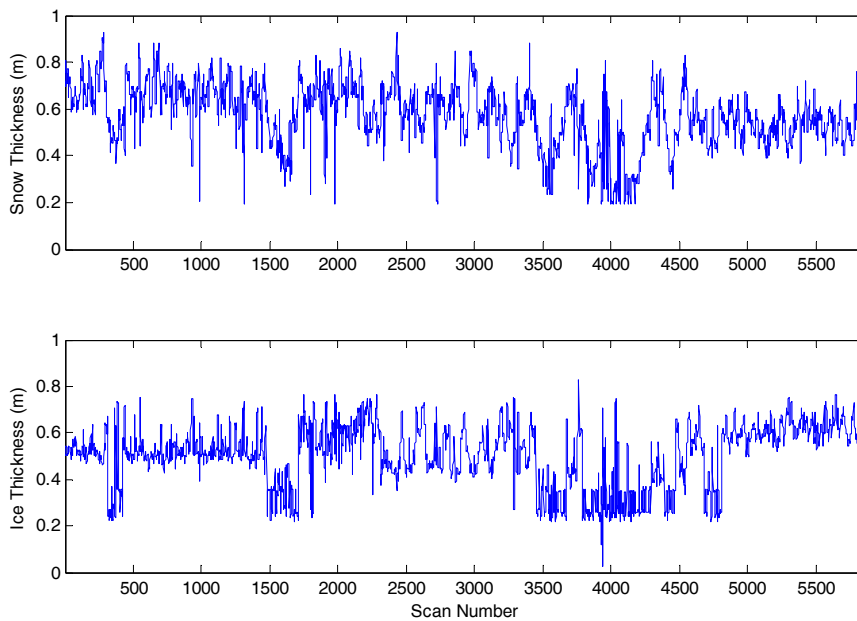


Figure 2.3 - Snow and ice thickness plots for the Lake Melville profile (Figure 2.2)

6

To enhance the viewing of the long profile, processing was performed to remove the helicopter height variations by aligning the GPR scans to the echo that was detected as the top of ice. The results of this processing are shown in Figure 2.4. Variation in the snow cover and ice thickness are now more readily seen. A clue to indicate that there may be brackish ice in this area of Lake Melville can be seen in the vicinity of scan numbers 400 and 1500. The GPR echo from the snow to ice interface becomes stronger over these sections and there is ringing seen below the snow to ice interface; these effects are common over brackish ice.

The report [3] on the 2009 Labrador survey includes GPR plots from Grand Lake, a nearby fresh water lake. The strength of the GPR echoes from the bottom of the ice in the Grand Lake plots looks similar to the echoes from the bottom of the ice echoes in Lake Melville where the ice is expected to be formed from fresh water.
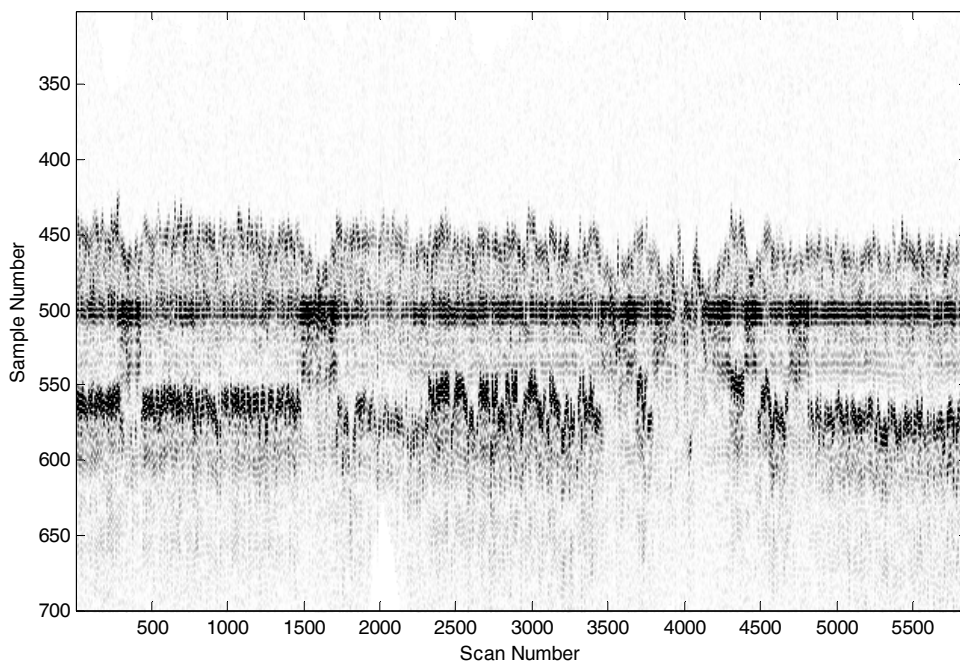


Figure 2.4 - Lake Melville GPR profile aligned using the detected top of ice echo.

## 2.2   GPR PLOTS OVER ICE WITH CHANGING SALINITY

The following plots (collected east of GPR line 854) show a change in ice salinity from fresh water ice to brackish water ice in the GPR profiles moving in a direction from west to east down Lake Melville. For GPR line 583, the echo from the ice water interface is greatly diminished once the ice becomes brackish. Surface sampling nearest to the end of line 583 is at Site 3. It will be shown that the GPR plot over site 3 is similar to the GPR plot from the end of line 583.
Table 1 shows the surface sampling performed at 3 locations on Lake Melville. The brackish water content of the ice was determined by making salinity measurement of ice chips taken at the 3 sites. Knowing ahead of time what the ice thickness is, guides the GPR interpreter to the location in the plot where the weak ice to water echoes should be located. Otherwise, there would be no clue

where to look given the high variability of the GPR echoes. The term clutter is used when many unwanted echoes hide the signal of interest.

Table 1 - Lake Melville on-ice station data (March 2009).

|  | Stn. 21-3 | Stn. 21-2 | Stn. 21-1 |
|---|---|---|---|
| Lat. (°N) | 53.77 | 53.92 | 54.038 |
| Long. (°W) | 59.422 | 59.041 | 58.578 |
| Time (EDT) | 15:15 | 14:30 | 13:30 |
| Snow depths (cm) E-W line | 56, 51, 38, **28**, 40, 54, 40 | 89, 60, 53, **48**, 50 48, 51 | 35, 33, 35, **45**, 19, 15, 20 |
| Snow depths (cm) S-N line | 70, 49, 60, **28**, 41, 50, 46 | 54, 59, 69, **48**, 55, 55, 65 | 30, 29, 18, **45**, 21, 20, 23 |
| Mean snow depth (cm) | 47 | 57 | 28 |
| Ice  (cm) | 158 | 98 | 79 |
| Freeboard (cm) | -4 | -1 | -10 |
| Salinity (at) | 8ppt (5cm) | 10ppt (5cm) | 8ppt  (5cm) |
| Salinity (at ) | 7ppt (48cm) | 12ppt (35cm) | 6ppt (29cm) |
| Salinity (at ) | --- | 9ppt (42cm) | 9ppt (45cm) |
| Surface water from CTD | 2.0ppt | 2.0ppt | 3.5ppt |
| GPR#  S-N | 580 | 574 | 570 |
| GPR# E-W | 579 | 575 | 569 |

### 2.2.1  *LINE 583 - TRANSITION FROM FRESHWATER TO BRACKISH ICE*

A 25 km long profile (GPR 583) collected on March 21 shows a transition from brackish ice to fresh water ice. For the last 5 percent of the profile (west end), the echo from the bottom of the ice is clearly seen (Figure 2.5). Figure 1.2 shows a Google Earth image locating the 3 sites and the long GPR profile 583.

Figure 2.5 shows a plot of a 1 km segment of the GPR profile 583 near the western end where the ice transitions from brackish to fresh water ice. On the right side (flying east to west) of the plot the fresh water ice thickness (ranging from 0.5 m to 0.7 m thick) can be readily seen.
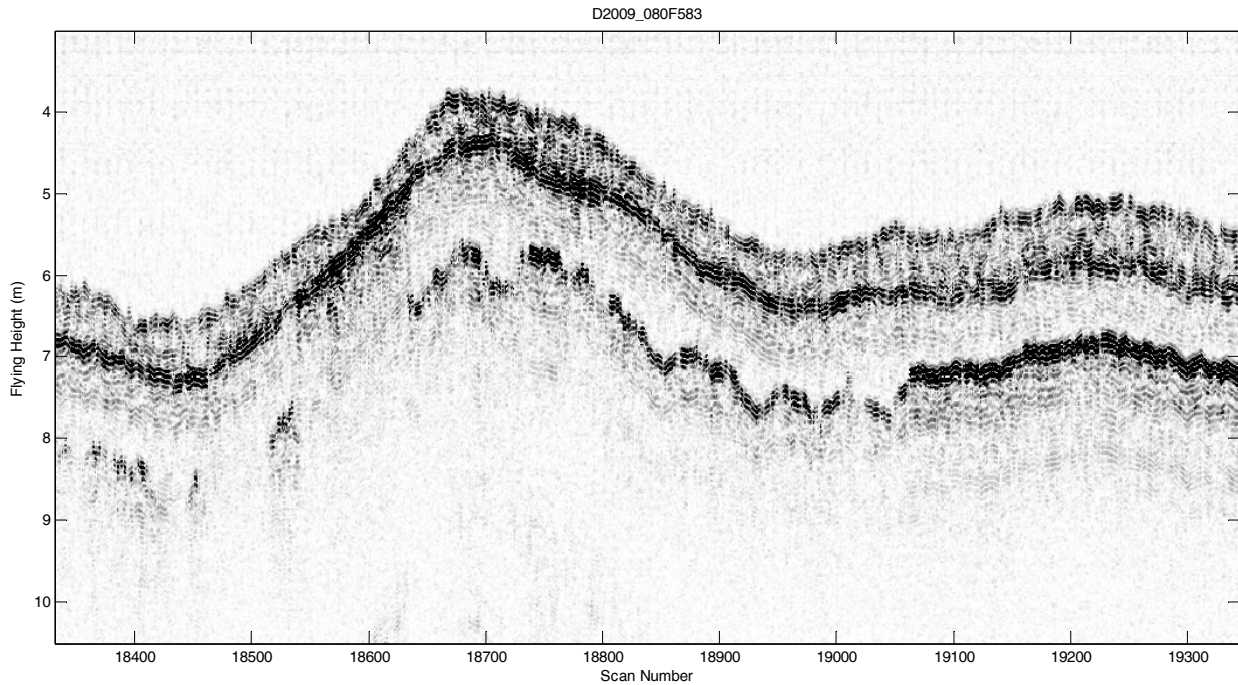
Figure 2.5 - A 1 km segment of the western end of GPR line 583.

Figure 2.6 shows a plot of a 1 km segment of GPR profile 583 near the eastern end where the ice is made from brackish water. The echoes from the ice to water interface are weak and intermittent. Figures 2.7 and 2.8 shown below for Site 3, have a few returns that might be from the ice to water interface at a similar depth as the weak ice echoes shown in Figure 2.6.
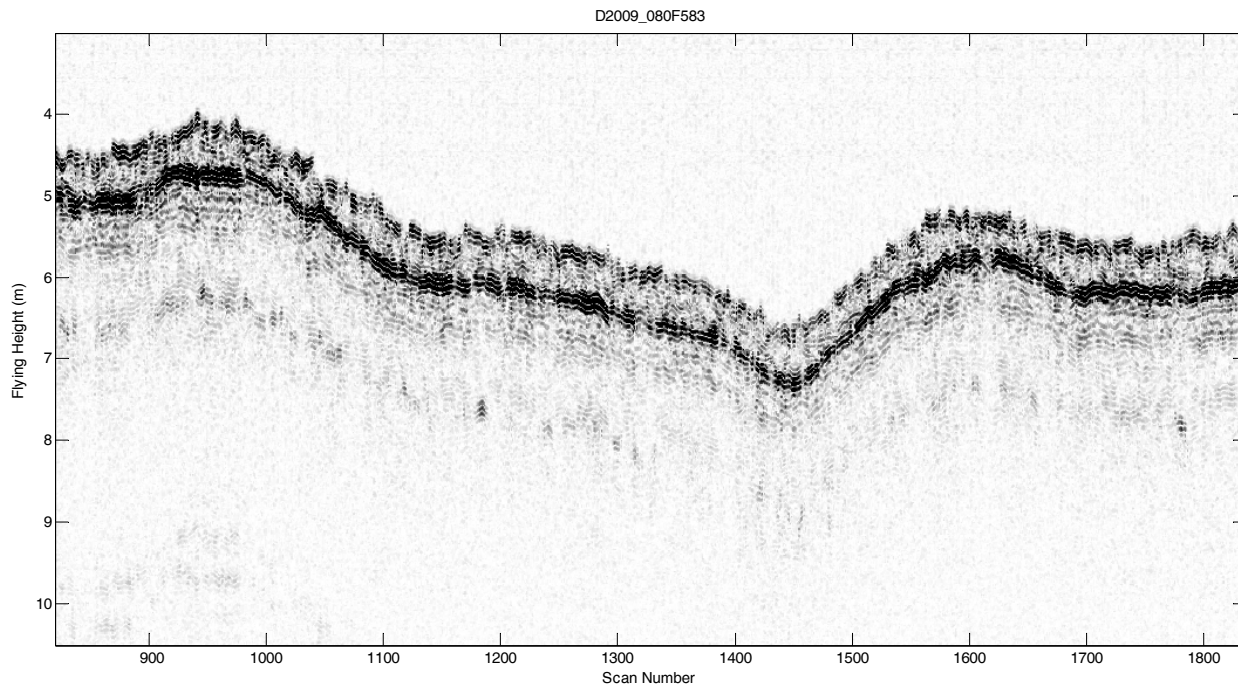


Figure 2.6 - A 1 km segment of the eastern end of GPR line 583 showing weak ice/water echoes.

## 2.2.2  THIRD SITE (21-3) ON LAKE MELVILLE

E-W and S-N GPR profiles were flown at this site, centered at the location where on-ice station data was collected (GPS coordinates: 53.7745N and 59.422W). Table 1 lists the surface sampling results for Site 3. GPR profile number 579 (shown in Figure 2.7) was flown east to west and GPR profile number 580 (shown in Figure 2.8) was flown south to north.

The blue circles in Figures 2.7 and 2.8 show echoes that are likely from the ice to water interface. This interpretation can be made given the availability of GPR line 584 which showed the transition from freshwater to brackish ice and the ice thickness auger hole. Even with this a priori information about the ice it is possible that the echoes in the blue circles come from other reflectors such as rubble on the surface off to the side of the helicopter. Average GPR derived snow depths range from 35cm to 45cm with values reaching up to 50cm.

Appendix A shows additional processing steps used to bring out the weak echoes from the ice to water interface for the GPR lines collected at Site 3 and Site 2. The approach taken is to remove the helicopter height variations from the GPR data so that along track averaging can be used to increase the signal-to-noise ratio of the ice to water echoes.
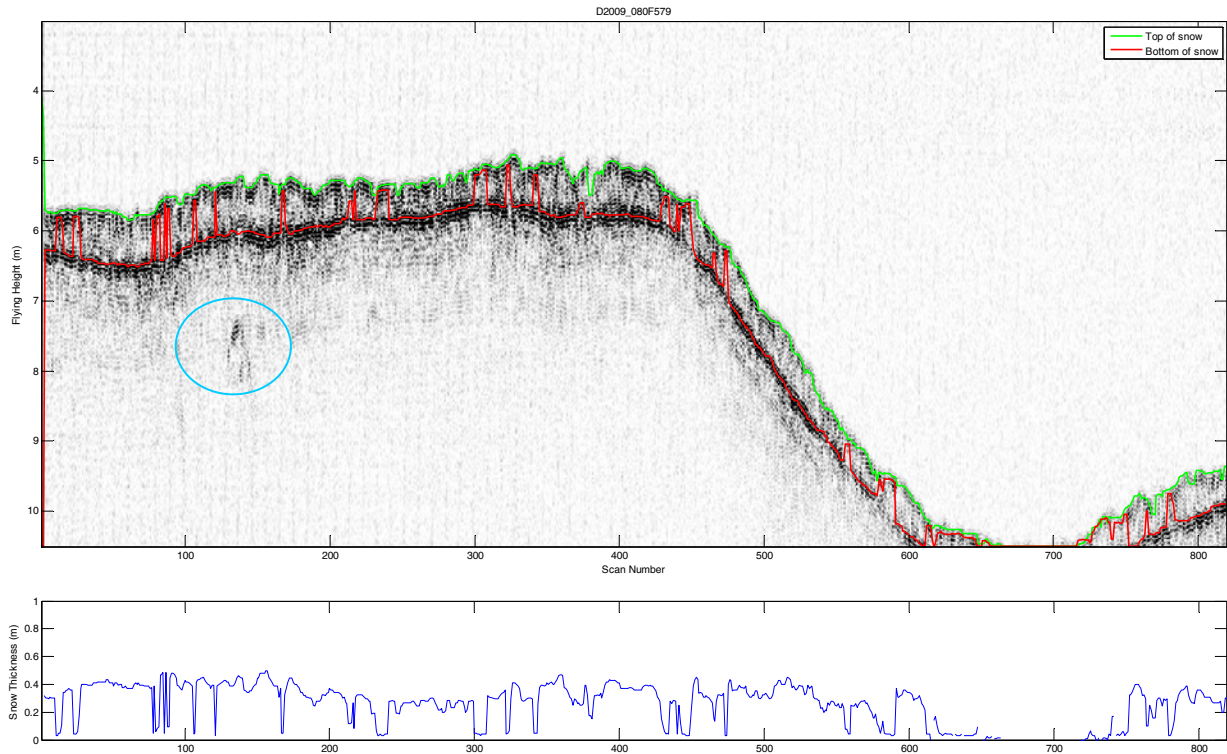


Figure 2.7 - GPR line plot and snow depth of third Site 21-3 GPR 579 line flown east to west.
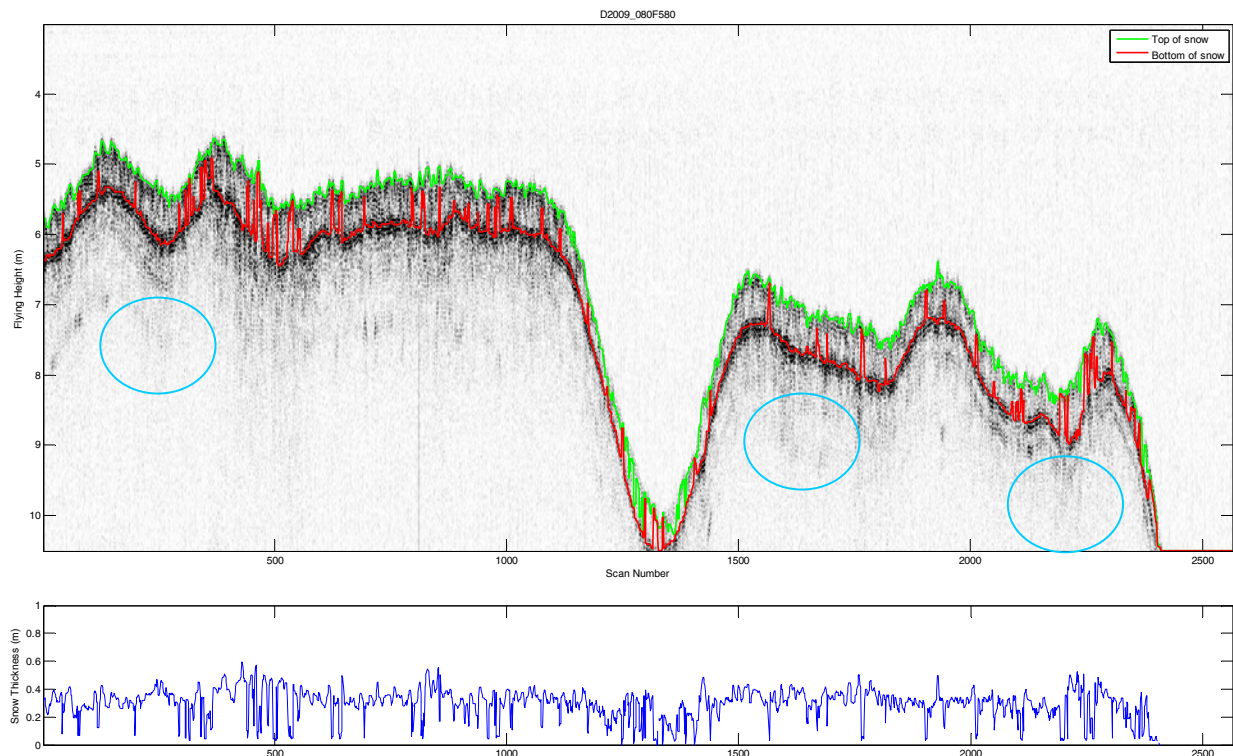
Figure 2.8 - GPR line plot and snow depth of third Site 21-3 GPR 580 line flown south to north.

### 2.2.3  SECOND SITE (21-2) ON LAKE MELVILLE

At the second site on-ice snow depths were larger than observed at the third site (21-3). E-W and S-N GPR profiles were flown at this site, centered at the location were on-ice station data was collected (GPS coordinates: 53.919N and 59.041W). Table 1 lists the surface sampling results for Site 2. GPR profile number 574 (shown in Figure 2.9) was flown south to north and GPR profile number 580 (shown in Figure 2.10) was flown east to west. The GPR derived snow depths were larger than those seen at the third site and reached at times over 60cm as seen in the on-ice data (Table 1).

These plots do not show any echoes that one could confidently report were from the ice to water interface. Extra processing shown in Appendix A was used to bring out the weak echoes from the ice to water interface. Plots A.5 and A.7 do show a likely echo for the ice to water interface for GPR line 574.
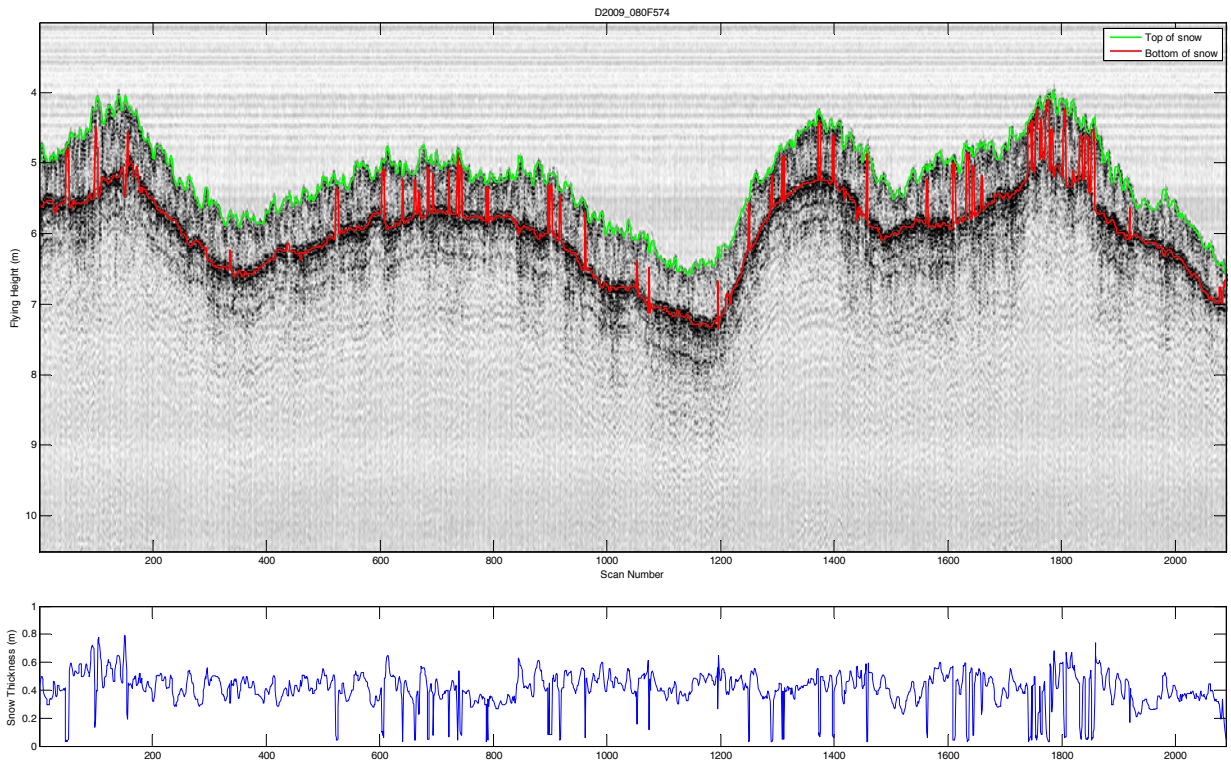
Figure 2.9 - GPR line plot and snow depth of second Site 21-2 GPR 574 line flown south to north.
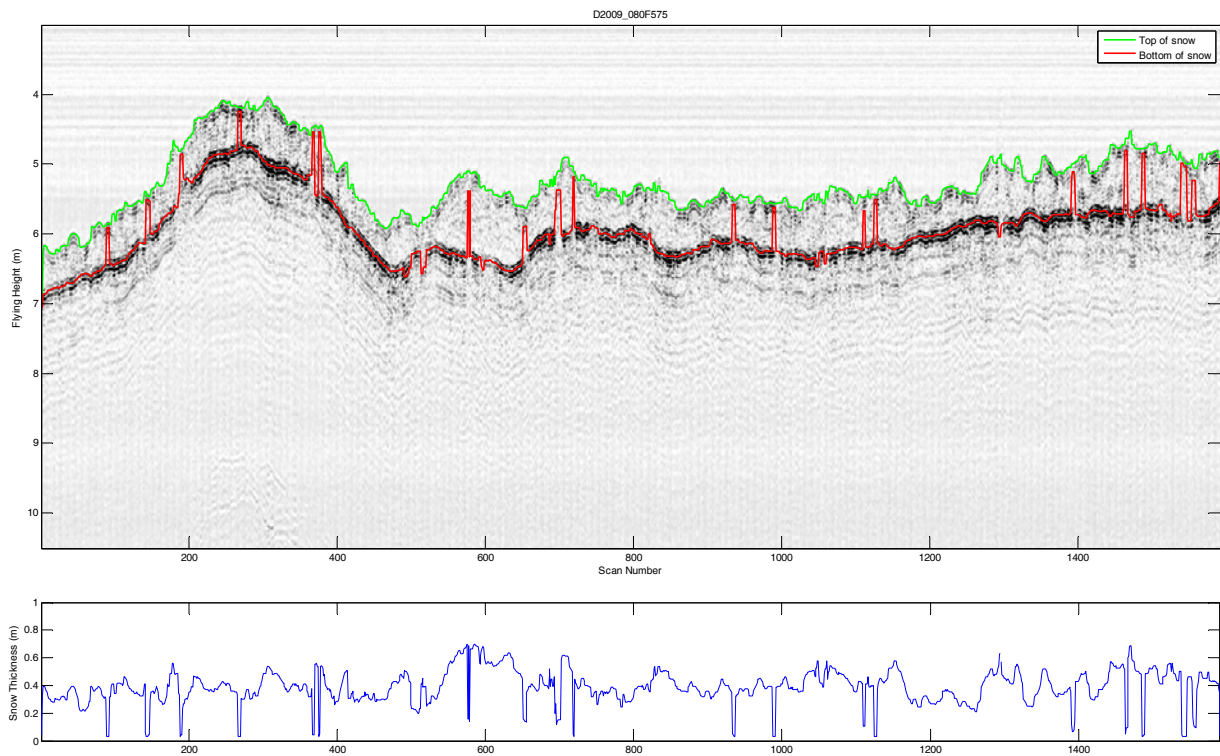


Figure 2.10 - GPR line plot and snow depth of Second Site 21-2 GPR 575 line flown east to west.

### 2.2.4 FIRST SITE (21-1) ON LAKE MELVILLE

The first site (21-1) was located just inshore (west) of the open water region of the narrow entrance of Lake Melville. E-W and S-N GPR profiles were collected at this site, centered at the location were on-ice station data was collected (GPS coordinates: 54.038N and 58.5776W). Table 1 lists the surface sampling results for Site 1. GPR profile number 569 (shown in Figure 2.11) was flown east to west; from the open water area where little snow was present to and just past the first site (21-1). The second GPR profile number 570 (shown in Figure 2.12) was collected while flying south to north. On-ice data sampling showed that snow thicknesses were less (28cm average, Table 1) than those seen at the other two sites farther away from the open water region. Figure 2.11 clearly shows the increase in snow thickness as one flew away from the open water region where the blowing snow was continually lost into the open water.

The blue circle on the right hand side of Figure 2.11 shows a possible echo from the ice to water interface though both Figure 2.11 and Figure 2.12 show very few under-ice echoes. The weak ringing that appears on the left hand side of Figure 2.12 (under the snow and ice surface) would indicate that the ice has electrical conductivity values higher than the other brackish ice in the area.
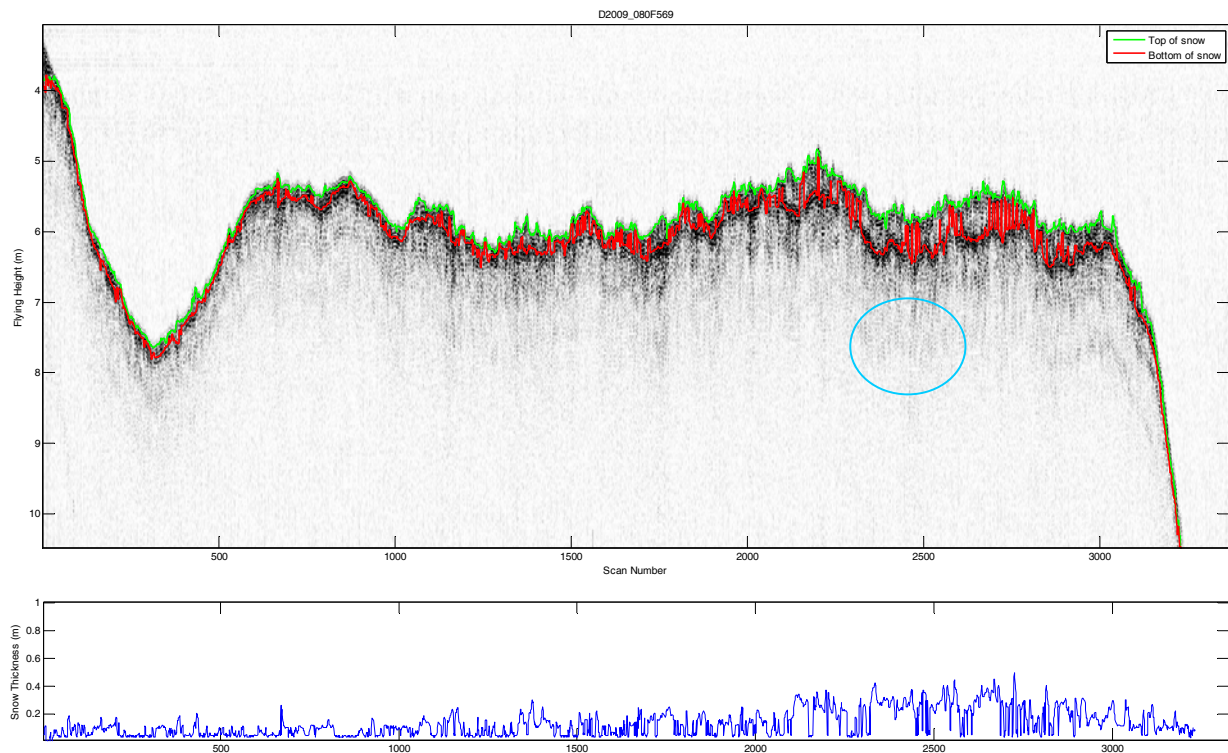


Figure 2.11 - GPR line plot and snow depth of First Site 21-1 GPR 569 line flown east to west.
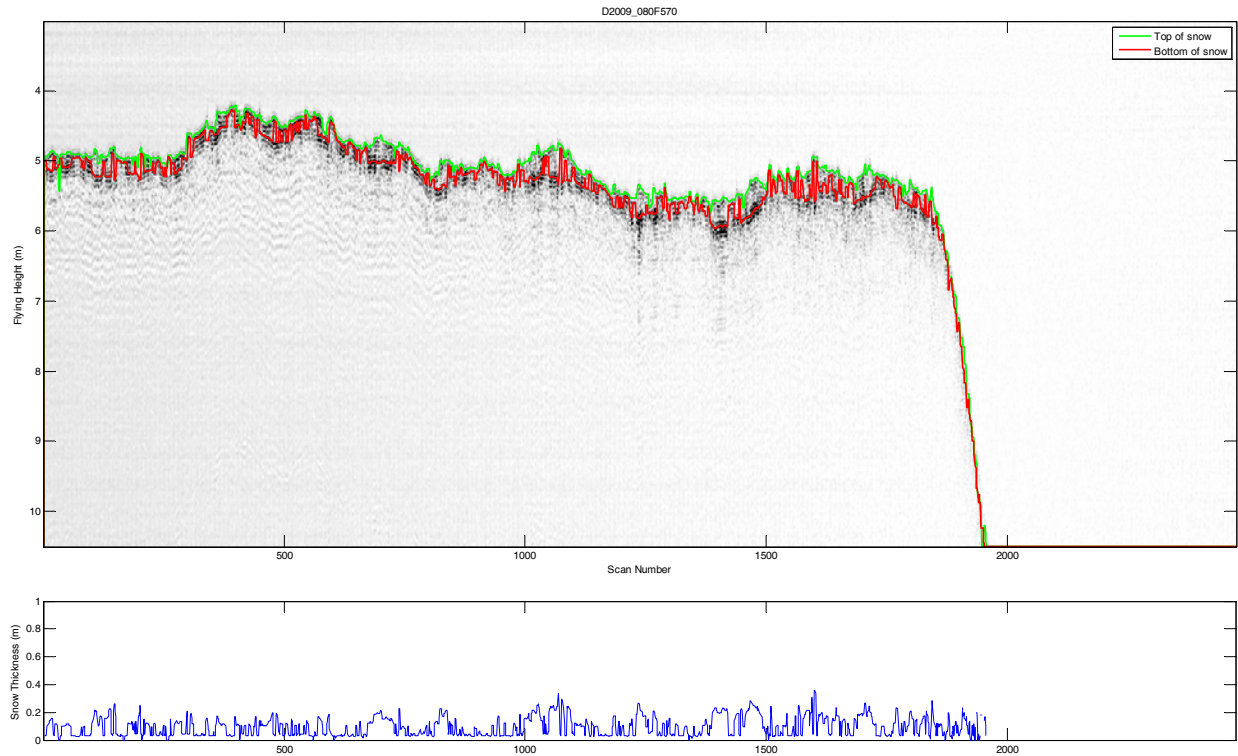
Figure 2.12 - GPR line plot and snow depth of First Site 21-1 GPR 570 line flown south to north.

## 2.3 COMPARISON OF THE NOGGIN 500 WITH THE NOGGIN 1000

The GPR data presented in the previous sections were collected using the Noggin 1000 GPR manufactured by Sensors and Software of Mississauga, Ontario. Also available from Sensors and Software is the Noggin 500 GPR system. Key differences between the Noggin 500 and the Noggin 1000 are:

- The Noggin 500 operates with a center frequency of 500 MHz versus the 1000 MHz for the Noggin 1000. The lower center frequency results in a longer pulse, thereby providing lower resolution.
- The Noggin 500 has a larger antenna area than the Noggin 1000 for increased sensitivity. This indicates that the Noggin 500 which would likely penetrate through a thicker layer of ice with a given brackishness than the Noggin 1000 and that the Noggin 500 would penetrate ice of a given thickness that has greater salinity than the Noggin 1000.
- The Noggin 500's dimensions are 39 cm long by 22 cm wide by 16 cm tall versus the Noggin 1000 which is 30 cm long by 15 cm wide by 12 cm tall. Both units will fit in the pod certified for air-borne survey work for the BO105 helicopter.

The February 2010 PEI survey did test flights with both the Noggin 1000 and Noggin 500 over fresh and brackish ice at several areas located in Prince Edward Island. Warm weather encountered during the data collection period did not provide good snow and ice conditions for GPR testing so conclusive results on the performance of the Noggin 500 versus the Noggin 1000 were not obtained.

Data plots for both the Noggin 1000 and Noggin 500 units are shown over "Radar Lake" [2]. Plots at several locations along the Hillsborough River are provided starting well up river and moving downstream.

### 2.3.1 FRESHWATER LAKE PLOTS

The flight tracks for the Noggin 1000 and Noggin 500 surveys are shown in Figure 1.3. GPR line number 603 used the Noggin 1000. GPR line number 635 used the Noggin 500. Figure 2.13 shows a 1 km section of the first half of an east-to-west flight over a freshwater lake using the Noggin 1000. Figure 2.14 shows a 1 km section of the first half of an east-to-west flight over a freshwater lake using the Noggin 500.

The above-ice conditions were very wet making the interpretation of the GPR profiles difficult. An auger hole was drilled in the middle of lake showed ice thickness of 35cm. There was 18 cm of very wet slush over the ice with 2 cm of wet snow above the slush. The expected two-way travel time through the 35 cm of ice is 4.6 ns (nanoseconds). The unknown is the velocity of the GPR through the slush. If the 18 cm of wet slush is essentially water then the two-way travel time through 18 cm of water is 10.8 ns. The y-axis for the following plots shows the flying height in air. The 1 meter tick marks represent a 2-way travel time of 6.6 ns. The subsurface echo seen at scan number 1000 in Figure 2.13 is approximately 8 ns below the top echo. So if the two-way travel time through the ice is 4.6 ns and the total time through slush and ice is 8 ns - that leaves 3.4 ns for travel through the 18 cm slush for a velocity in slush of 0.016 m/ns. A velocity of 0.016 m/ns would indicate a dielectric constant of 8 for the slush - much higher than the maximum for ice (4) and well above the range of the typical dielectric value for dry snow (1.5).

With the information available from the Noggin 1000 interpretation, the first strong subsurface echo in Noggin 500 plot shown in Figure 2.14 is likely from the ice/water interface.

There are several areas in Figure 2.13 where drier surface snow may be visible with the Noggin 1000. The top echoes near scan numbers 370, 650 and 900 look like they are from surface snow. There is very little snow echo seen with the Noggin 500 in Figure 2.14;  the area of scan number 500 there is a very small echo that is probably from the drier snow layer. The lower resolution of the Noggin 500 make interpretation of the GPR returns very difficult.
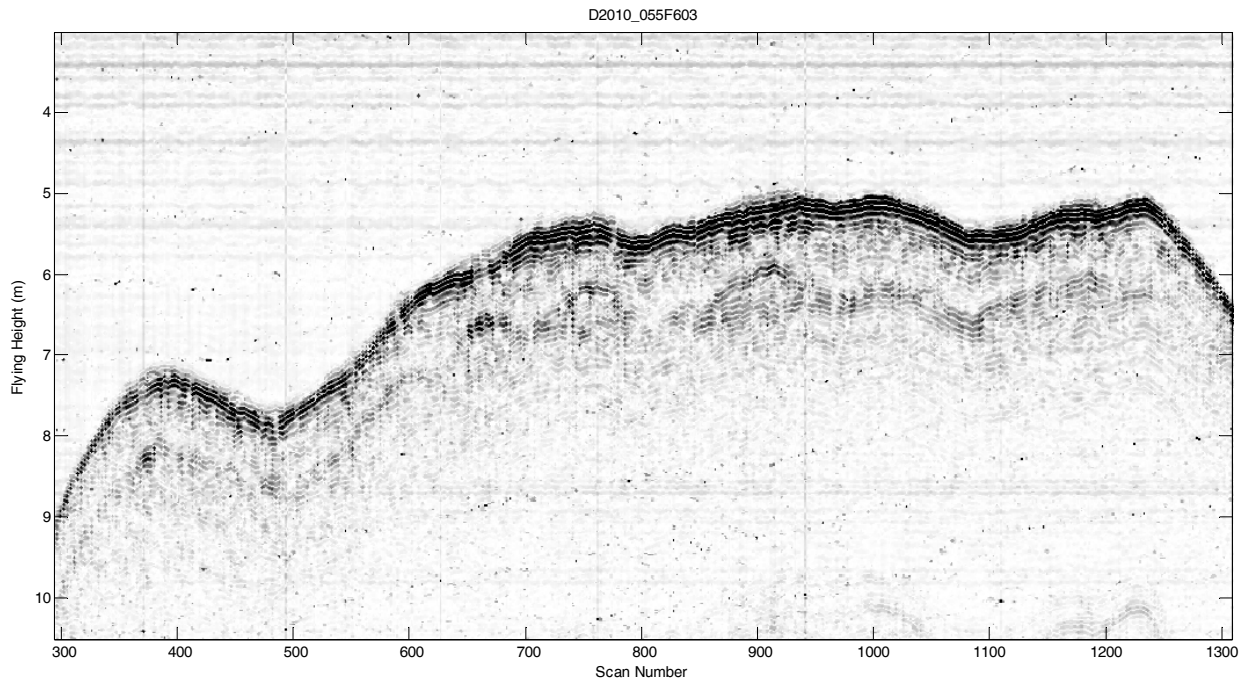
Figure 2.13 - A plot Noggin 1000 GPR data for a 1 km section of the first half of an east-to-west flight over the freshwater lake
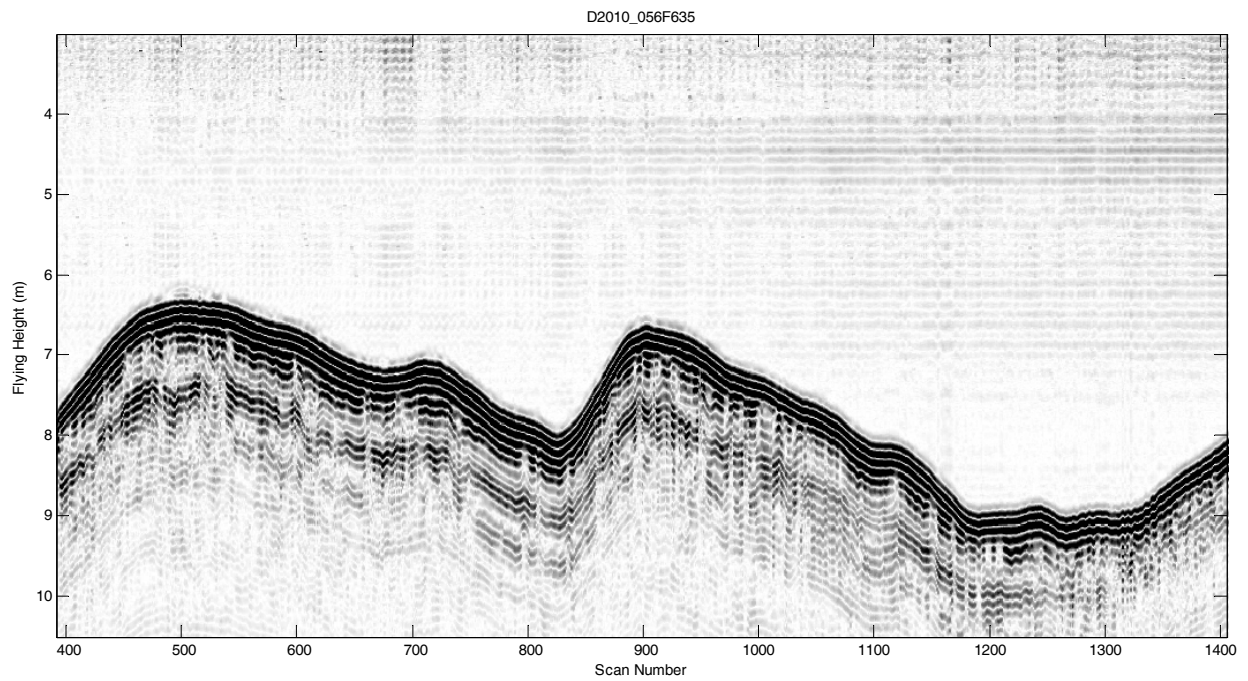


Figure 2.14 - A plot Noggin 500 GPR data for a 1 km section of the first half of an east-to-west flight over the freshwater lake

## 2.3.2 HILLSBOROUGH RIVER PLOTS

Figure 1.4 shows the tracks for three Noggin 500 GPR lines taken over the ice covered Hillsborough River. Line 633 was collected at the farthest upstream location and a 1 km section is shown in Figure 2.15. Figure 2.16 shows a 1 km section for line 631 which was collected midway upstream and Figure 2.17 shows a 1 km section collected near the City of Charlottetown. The Hillsborough River flows into the salt water Northumberland Strait so the water in the river is expected to be brackish some of the time.

An auger hole was drilled in the river ice at a location near the start of line 633. It showed ice thickness of 20cm with 18 cm of very wet slush over the ice. The expected two-way travel time through the 20 cm of ice is 2.6 ns (nanoseconds). If the 18 cm of wet slush has the same dielectric constant as the slush at Radar Lake, then the two way travel time though the slush is 3.4 ns. The expected return echo from the ice/water interface is 6 ns below the top echo - which corresponds (approximately) to the 1 m y-axis tick separation.

There is an echo in the plots over the river that would be a good candidate for the ice/water interface. All three plots have a lot of ringing which typically indicated that the surface material is conductive. There is ringing at approximately the same location as the expected ice/water interface echo. The addition of the echo from the ice/water interface and the ringing creates interference and phase change in the echoes. The GPR plot shown in Figure 2.15 shows a few clues to the presence of the ice/water interface echo by small shifts or phase changes in the ringing in the vicinity of scans 720 to 780, from scans 850 to 890 and around scan 1200.

The subsurface echoes seen in the Hillsborough River plots have a weaker intensity that the freshwater GPR survey at Radar Lake. Moving downstream from Figure 2.15 to Figure 2.16 to Figure 2.17, the subsurface echoes get progressively weaker.
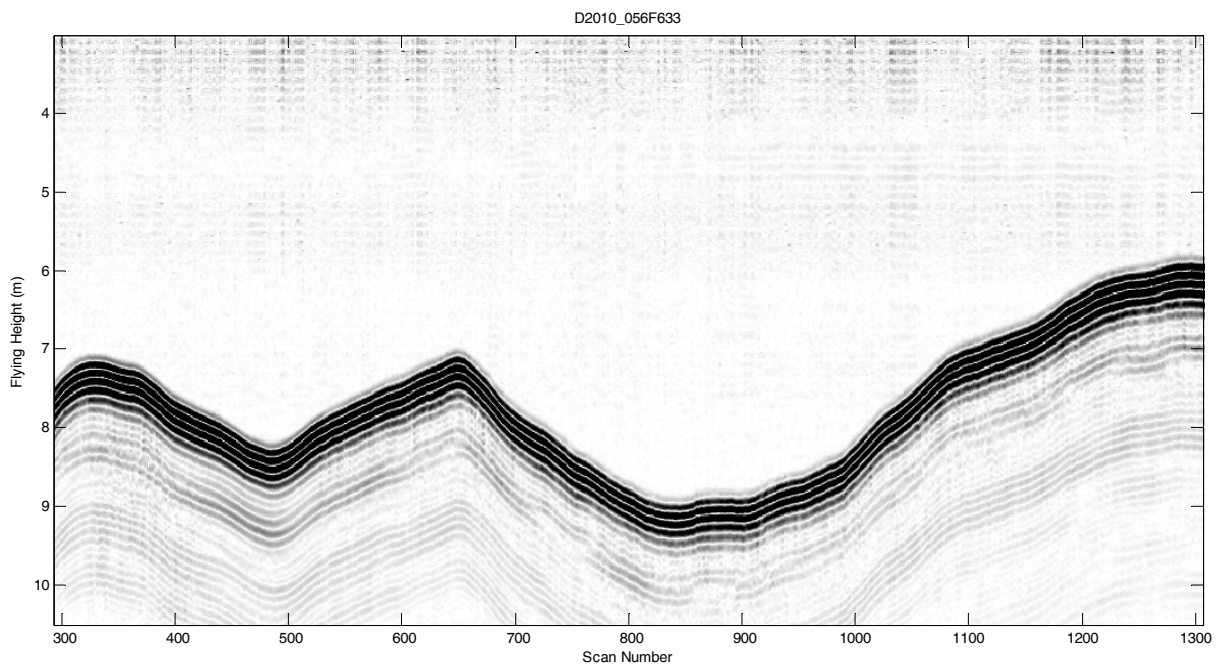


Figure 2.15 - A plot Noggin 500 GPR data for a 1 km section of the upstream location on Hillsborough River

D2010_056F631
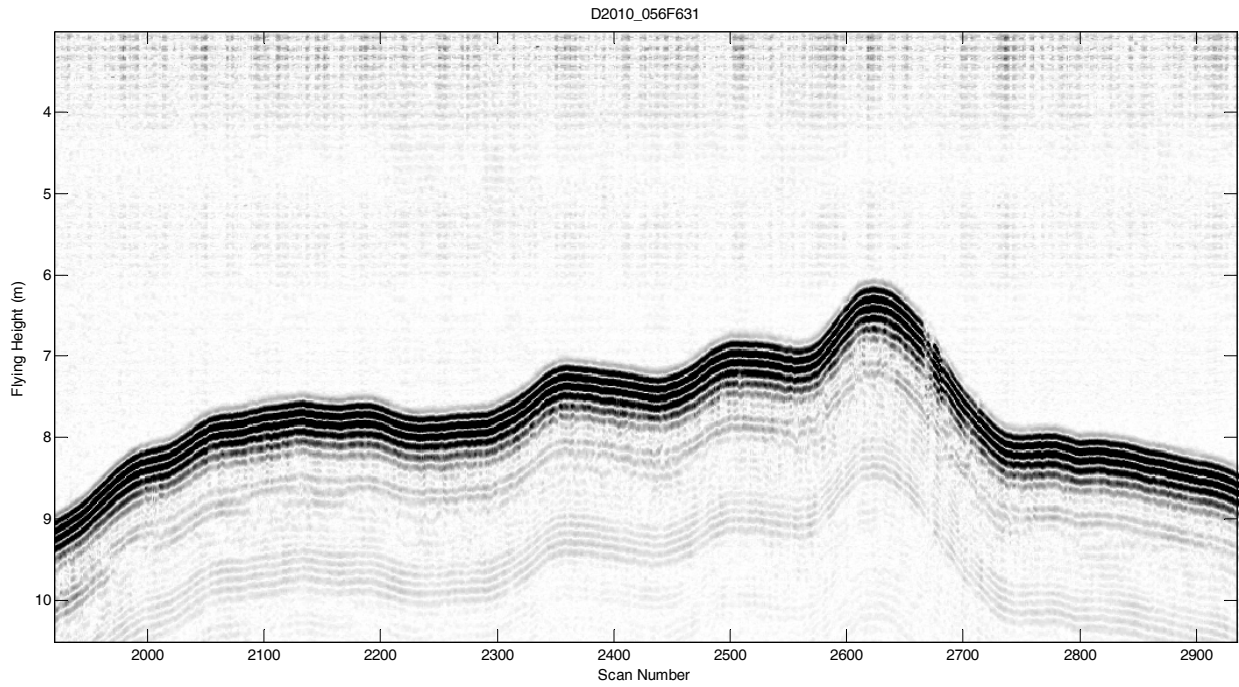
Figure 2.16 - A plot Noggin 500 GPR data for a 1 km section of the midway upstream location on Hillsborough River

D2010_056F629
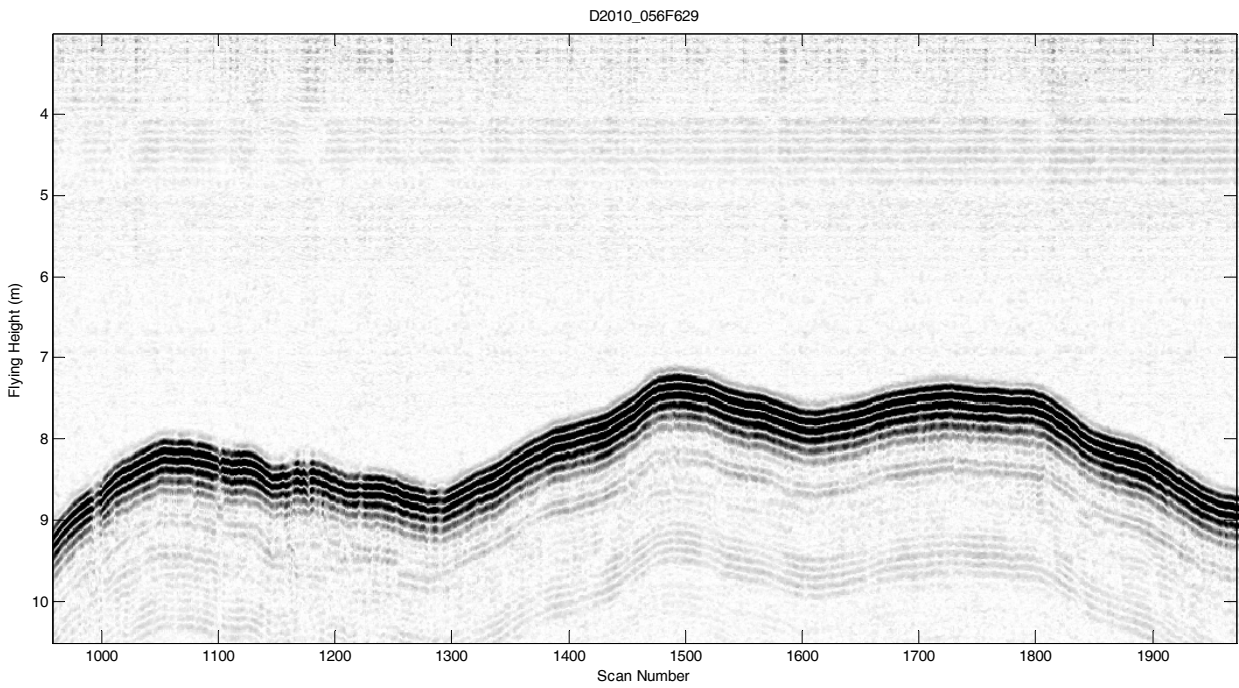
Figure 2.17 - A plot Noggin 500 GPR data for a 1 km section of the downstream location on Hillsborough River

# 3   OIL-IN-ICE DETECTION

This section provides a report on the likely success for the use of the BIO helicopter-borne GPR for the detection of oil-in-ice. The following items are covered in this section:
- Dickens/Boise Oil-In-Ice Development
- Overview on GPR Usage
- Anomaly Detection
- Possible Approach for Oil Detection

The author presumes that the goal for a sensor to detect oil-in-ice would be suitable for use by non-GPR experts and that automated processing would be performed using sensor data to provide an oil-no-oil indicator to the system operator.


## 3.1   DICKENS/BOISE OIL-IN-ICE DEVELOPMENT

One group that has been actively pursuing the development of GPR for oil-in-ice detection is the group is lead by David Dickens of DF Dickens and Associates of La Jolla, California.


### 3.1.1   EXCERPTS FROM THE U.S. GOVERNMENTS BUREAU OF OCEAN ENERGY MANAGEMENT, REGULATION AND ENFORCEMENT WEBSITE AND REPORTS

From http://www.boemre.gov/tarprojects/569.htm:

"From March 27-31, 2006, the ground penetrating radar successfully detected and mapped the oil from the surface, showing a clear difference in signature between clean and oiled ice."

From: http://www.boemre.gov/tarprojects/588.htm

"The current generation GPR is capable of mapping oil under or trapped within growing winter ice from 30-210 cm (1-7 foot thick). Minimum oil thickness detection limit appears to be roughly 2cm."

Paraphrasing the Phase 2 report [4]:

- Reports success with surface GPR for oil-in-ice detection
- No success with airborne yet
- Conclusion is that ground GPR usage may reduce augering for the detection of oil-in-ice

Page iii of the report states "Surface-based ground penetrating radar (GPR) operating at 500 MHz clearly delineates changes at the ice water interface caused by emplacement of oil".

Page 27 of the Phase 2 report shows plots of ground-based GPR data before and after oil emplacement. Page 32 shows an airborne GPR plot.

Paraphrasing the Phase 3 report [5]:

- Reports that GPR is capable of detecting oil-in-ice
- Reports that GPR is not useful for detecting the thickness of the oil layer
- Mentions that a minimum oil layer thickness of 2 cm is required for detecting oil-in-ice

While the above detection of oil-in-ice are impressive results, this author is of the opinion that if the interpreter did not know the thickness of the ice or where in the profile to look for the oil induced anomaly, then the amount of variability in the GPR returns would produce a low probability for detecting the oil. The next section discusses GPR and possible issues with the premise used by Dickens's group of the detection of oil-in-ice.


## 3.2 THE DIFFERENCE BETWEEN GPR THICKNESS MEASUREMENT AND ANOMALY DETECTION

GPR used for snow or ice thickness measurement uses the time difference of arrival of GPR echoes to determine the layer thickness. This technique uses signal processing to detecting the GPR echoes, pick the echoes for the top of the layer and the bottom of the layer and report the thickness. GPR layer thickness measurement is robust to amplitude changes of the GPR echoes.

Large variations in amplitude and phase of the echo from the bottom of the ice are a regular occurrence in GPR data and the author expects that the mapping the amplitude and/or phase of the echo from the bottom of the ice would produced a white noise plot.


### 3.2.1 OVERVIEW ON GPR

The GPR transmitter sends out a very short radio frequency (RF) pulse. The pulse will both reflect off and penetrate into the surface layers, in this case snow and ice.

With an airborne system, the GPR pulse starts off in the air and first encounters the air-to-snow interface. Some of the pulse's energy will reflect back to the GPR and some penetrate the snow. The next interface for the penetrating pulse is from the snow-to-ice interface. Again some energy will reflect back to the GPR and some will penetrate the ice. The next possible interface for the penetrating pulse is from the ice-to-water interface. Some energy will reflect back and some will penetrate the water.

Sea water has high electrical conductivity which effectively stops the GPR pulse within the first few centimeters. The reflection of the GPR pulse off sea water is very strong which creates a reverberation (or ringing) of the GPR pulse - this shows up as a strong band of echoes - which can be seen near scan numbers 9100, and 9950 in Figure 27 of [3].

The key to GPR measurement of snow and ice thickness is that the measurement taken from the GPR signal is travel time. Electromagnetic waves like the GPR pulse travel at the speed of light. In air, the GPR pulse travels at the speed of light in free space (299762458 m/s). As GPR systems typically report time in nanoseconds, the free space speed used is 0.3 m/ns (or 1 foot per nanosecond). The dielectric constant of a material is used to calculate the speed of the GPR pulse in

different materials. For dry snow the dielectric constant can range from 1.2 to 1.5 and for ice (freshwater and sea water) the dielectric constant can range from 3.2 to 10 (from [6] and [7]). GPR velocity is determined by dividing the speed of light in free space by the square-root of the dielectric constant.

Given the variation in dielectric constant for snow and ice, either the in-situ snow and ice properties are measured or the GPR system is calibrated in the field by surveying over an area that has been hand-measured.

GPR systems provide clear easily interpretable data when flying over flat ice. When rubble and ridges are encountered the radar return becomes highly variable and the layers of snow and ice cannot be determined. Figures 13 and 40 in [8] provide example GPR plots where there are a number of layers encountered. While the top layer is likely snow, which layer is (or how many layers are) the ice? How would you know the top layer is snow if you were not there?

### 3.2.2   *AMPLITUDE VARIATIONS*

The amplitude of the GPR echo changes with varying flying height. The amplitude can also vary with the nature of the interface layer where the echo comes from. The interface layer can vary in the rate of change from one material to the other. The snow-to-ice interface layer can be abrupt if fresh snow has fallen on clear ice or the layer can be gradual if there has been a thaw.

### 3.2.3   *ANOMALY DETECTION OF AMPLITUDE VARIATIONS*

As mentioned above in Section 3.1, the Dickens/Boise oil-in-ice detection method looks for a signature;  a change in the amplitude or phase of the echo from the bottom of the ice. Detecting changes in the ice-to-water interface indicates that the technique to locate the oil is an anomaly detector, which is a viable technique if the expected false alarm rate is low. This differs from snow and ice thickness measurement where the travel time of the pulse through the snow and ice is used.

The premise to use anomaly mapping for GPR oil-in-ice detection is to locate variations in the ice-to-water interface caused by emplacement of oil. This requires a very good foreknowledge of the snow, ice and water conditions that will be encountered.

Who would be the end users of the sensor? Chances are slim that a GPR expert would be on hand when an oil spill occurs to interpret the results. Ideally, the expert would need to be in the field guiding the data collection.

There are scenarios where anomaly mapping for oil-in-ice using GPR is possible. First, the snow and ice properties should be determined. The ice conditions and ice thickness needs to be determined to indicate to the user the chance for GPR penetration. If the user knows there is a spill and users can find areas of common snow and ice conditions where oil is present and where there are oil free areas, then airborne profiles from the oil-free areas to the oil-in-ice areas can be flown. The user needs a training dataset to learn what the oil-in-ice anomaly will look like.

In the authors opinion though, in a blind test to locate oil-in-ice, there would not be any reasonable expectation that a GPR sensor would be successful. To increase the chance for success, other information and sensors are needed.

## 3.3 POSSIBLE APPROACH FOR OIL DETECTION

Some of the variables to consider:
- Is the snow dry or wet and how thick is it? Changing snow conditions can change the GPR signal penetration which would affect the amplitude of the snow-to-ice interface.
- How thick is the ice? The Dickens/Boise on-ice approach is reported to work with ice up to 7 feet thick. How do you know the ice is 7 feet or less?
- Is the ice first year sea ice, multi-year ice or freshwater ice? The GPR has different performance over each type.
- Is the ice rough? Under this conditions the bottom of the ice would not be detectable

If the above variables can be determined, then perhaps the false alarm rate of an anomaly detector can be reduced.

The BIO EIS-Pick EM ice thickness sensor can measure a wide range of ice thicknesses and measure ice and water conductivity. This sensor can help determine if the ice conditions where the oil spill has occurred conditions are amenable to the GPR oil-in-ice sensor.

An array based GPR hardware architecture might permit the measurement of both the layer velocity of the GPR signal in each layer and each layers the thickness, solving the problem of having to guess the dielectric constant of the snow and ice. Also a GPR hardware architecture that would add beam forming for footprint focusing and clutter removal would also help to reduce the variability of the GPR return.

# 4 CONCLUSIONS

The use of GPR for the thickness measurement of brackish ice has been demonstrated. The major difficulty with brackish ice thickness measurement is that the user would not likely know the salinity of the ice ahead of time whether or not the GPR would penetrate through the ice. Interpretation of brackish ice GPR plots was possible with surface sampling measurements. The use of the Noggin 500 would provide a higher probability of success with brackish ice thickness measurement at the cost of resolution;  the higher resolution provided by the Noggin 1000 makes interpretation of the GPR plots easier.

For the oil-in-ice problem, in the author's opinion, under ideal conditions, GPR could be used to detect oil by anomaly detection with a GPR expert interpreting the data. As a general tool for non-expert users to employ "an automated processing technique" with a simple GPR system would not

provide a reliable oil-in-ice detection system. Success may be possible with a joint technology system using various sensors to overcome the shortcomings of a stand-alone single GPR system.

# 5 References

[1] Lalumiere, L., 2006 Ground Penetrating Radar for Helicopter Snow and Ice Surveys. Can. Tech. Rep. Hydrogr. Ocean Sci. 248: iv + 44p.

[2] Lalumiere, L. and S.J. Prinsenberg, 2009. Integration of a Helicopter-Based Ground Penetrating Radar (GPR) with a Laser, Video and GPS System. Conf. proceedings, Int. Society of Offshore and Polar Engineering ISOPE-2009, Osaka, Japan, ISSN 1098-618: 658-665.

[3] Prinsenberg, S.J., I.K. Peterson, J.S. Holladay and L. Lalumiere, 2011. Labrador Shelf Pack Ice and Iceberg Survey, March 2009.  Can Tech. Rep. Hydrogr. Ocean Sci. 269: viii+76pp.

[4] 2006 Svalbard Experimental Spill to Study Spill Detection and Oil Behavior in Ice, Final Technical Report, DF Dickins Associated Ltd., SINTEF, The University Center in Svalbard, Boise State University, 55 pp., December 15, 2006. (http://www.boemre.gov/tarprojects/569/569AC.pdf)

[5] Dickins, D.F., Bradford, J. Detection of Oil On and Under Ice: Phase III: Evaluation of Airborne Radar System Capabilities in Selected Arctic Spill Scenarios. Final Technical Report  2008. (http://www.boemre.gov/tarprojects/588/GPR07Final.pdf)

[6] Ulriksen, P.: Application of impulse Radar to Civil Engineering, Doctoral Thesis, Lund university of Technology, Dept. of Eng. Geol., Sweden. Coden: Lutvdg/(TVTTG-1001)/1-175, 1982.

[7] Morey, R. M. 1975 "Airborne sea ice thickness profiling using an impulse radar" U.S. Coast Guard Technical Report No. CG-D-178-75.

[8] Prinsenberg, S.J., I.K. Peterson, J.S. Holladay and L. Lalumiere, 2010. Helicopter-borne sensors monitoring the pack ice properties of Mackenzie Delta: April 2010 Sea Ice Survey. Can Tech. Rep. Hydrogr. Ocean Sci. 267: viii+62pp.

**Appendix A - Extended Processing for the Lake Melville GPR Data**

**Summary**

GPR data from three sites at Lake Melville collected on March 21, 2009 were analyzed to determine if the bottom echoes of the brackish ice could be detected.

Processing was performed to remove the effect of helicopter flight variations and aligned the GPR data along the detected top of the ice echo. This aligned data then had a time varying gain applied and it was then smoothed to accentuate features that are parallel to the ice surface (perhaps the ice bottom) and attenuate features that clutter the GPR plot such as multiple echoes and surface scatterers.

Figures A.5 and A.10 show the best results for the Site 2 profiles. From the 2009 Labrador Sea Ice Survey, the Site 2 ice thickness is approximately 98 cm. This corresponds to 117 samples in the GPR data. From the plots, there is a consistent echo at approximately 100 samples below the top of ice echo.

Figures A.13 and A.16 show the results for the Site 3 profiles. From the 2009 Labrador Sea Ice Survey, the Site 3 ice thickness is approximately 158 cm. This corresponds to 188 samples in the GPR data. From the plots, there is a consistent echo at approximately 95 samples below the top of ice echo.

Site 1 profiles were not included in this analysis as the snow layer was very thin and the location of the ice surface was very poor.

A long profile over Lake Melville does show a transition from brackish ice to fresh water ice. The ice thickness at in the freshwater section at the end is similar to the echoes seen at Sites 2 and 3.

In conclusion, it appears that the GPR data from over the brackish ice of Lake Melville does have some echoes from within the ice but there is uncertainty whether or not the bottom of the ice was detected.

**Introduction**

GPR data from three sites at Lake Melville collected on March 21, 2009:

- Site 1: GPR files D2009_080F569 and D2009_080F570
- Site 2: GPR files D2009_080F574 and D2009_080F575
- Site 3: GPR files D2009_080F579 and D2009_080F580

From the Labrador Sea Ice Survey 2009 technical report (3), the approximate snow and ice thicknesses were listed as follows:

- Site 1: snow 45 cm, ice 79 cm
- Site 2: snow 48 cm, ice 98 cm
- Site 3: snow 28 cm, ice 158 cm

This note describes the processing developed and applied to determine if the Noggin 1000 GPR can penetrate the brackish ice of Lake Melville.

The following processing functions were applied:

- remove outliers to smooth the location of the bottom of the snow (top of the ice)
- Use the location of the top of the ice to align the GPR data so that the ice echo appears as a straight line across the plot
- Apply a running average filter to the ice-echo aligned data
- Apply a time-varying gain function to the ice-echo aligned data
    - Apply the running average
- Apply an automatic-gain-control (AGC) function
    - Apply the running average

**Processing Steps**

The snow thickness processing algorithm provides the location of the top of the snow and the bottom of the snow over sea ice. Generally, the GPR signal has little or no penetration into the sea ice. Plots of the GPR data from the 3 sites at Lake Melville do show some echoes from below the ice surface. While these echoes come at a later time than the ice surface, they could come from multiple reflections or from other side echoes.

Gain functions can be used to bring up small echoes but they are only useful if GPR clutter echoes (side echoes and multiple reflections) and random noise are can be reduced.

Using the location of the top of the ice from the snow thickness processing, it is possible to align the GPR data to so that it can be plotted with the top of ice echo as a straight line across the plot. With the ice echo as a straight line, a running average filter will remove features that are not parallel to the ice surface.

**Expected GPR travel time through ice and snow**

To convert GPR echo times to snow or ice thickness, a choice for the dielectric constant (k) needs to be selected (or estimated using ground truth data).

For dry snow, k has been selected to be 1.5 guessing that the snow was very dry. For ice, k has been selected to be 3.2 out of a range from 3.2 to 4. Choosing 3.2 is biased to provide a shorter travel time through the ice.

The GPR measures two-way travel time. The two-way travel time for a given snow or ice thickness is calculated as follows:

Thickness = c/sqrt(k) where c is the speed of light (.299792458 m/ns)

Two-way travel times:
Site 1:
- snow 45 cm: 3.67 ns
- ice 79 cm: 9.42 ns

Site 2:
- snow 48 cm: 3.92 ns
- ice 98 cm: 11.69 ns

Site 3:
- snow 28 cm: 2.29 ns
- ice 158 cm: 18.84 ns

Converting two-way travel times to GPR samples at 0.1 ns per sample:
Site 1:
- snow 45 cm: 37 samples
- ice 79 cm: 94 samples

Site 2:
- snow 48 cm: 39 samples
- ice 98 cm: 117 samples

Site 3:
- snow 28 cm: 23 samples
- ice 158 cm: 188 samples

Site 2 – GPR Profile #574

Replot and re-application of snow thickness processing. Processing steps applied for the plot shown in Figure A.1 are as follows:
- De-bias each individual GPR scan by subtracting an average of the first 50 points
- Bandpass filter using a 3rd order butterworth filter applied using Matlab's filtfilt routine producing 3dB cutoff frequencies of 500 MHz and 1500 MHz.
- Apply 1-dimensional snow thickness processing and remove the outliers to smooth the location of the bottom of the snow (top of the ice)
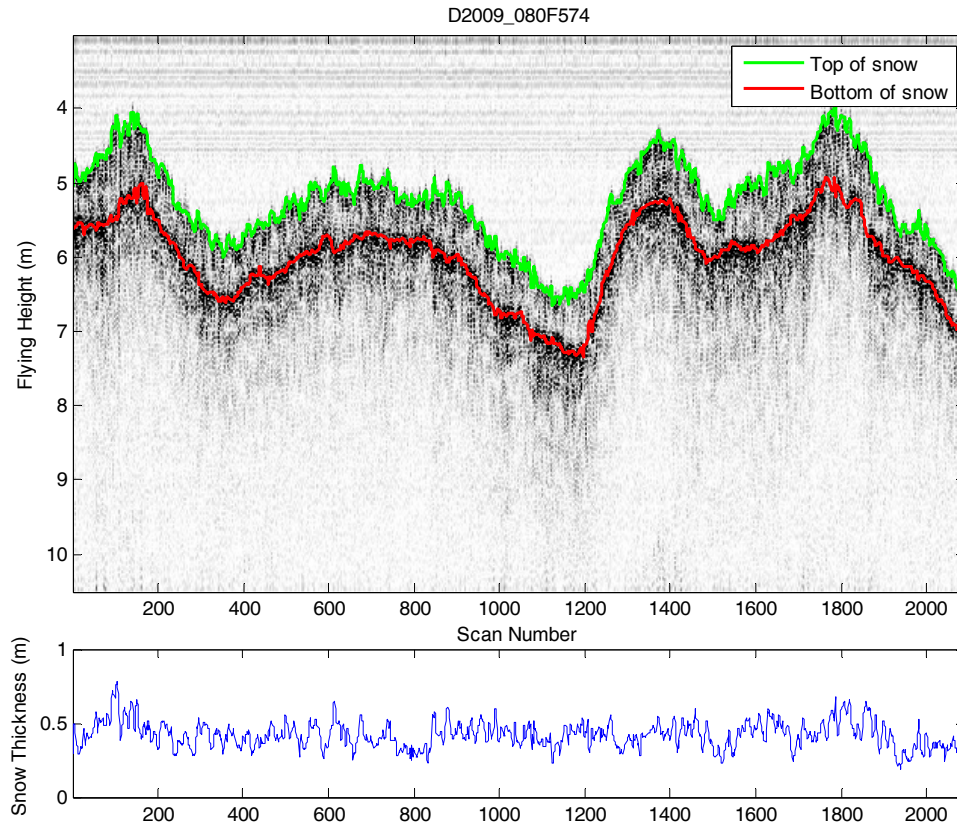
Figure A.1 Site 2 GPR Profile #574 data plot and snow thickness result

The following plots with the additional processing functions for Site 2 GPR Profile #574 are as follows:

- Figure A.2 - Use the location of the top of the ice to align the GPR data so that the ice echo appears as a straight line across the plot
- Figure A.3 - Apply a running average filter to the ice-echo aligned data
- Figure A.4 - Apply a time-varying gain function to the ice-echo aligned data
- Figure A.5 - Apply the running average to data with time-varying gain applied
- Figure A.6 - Apply an automatic-gain-control (AGC) function
- Figure A.7 - Apply the running average to data with AGC applied
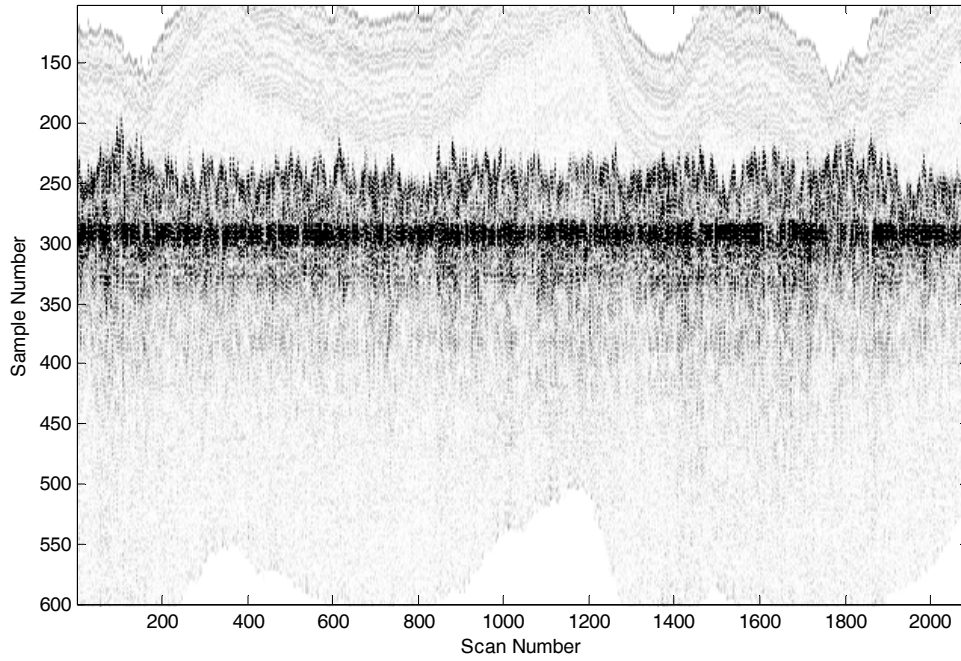
Figure A.2 GPR Profile #574 aligned to flatten out the ice echo
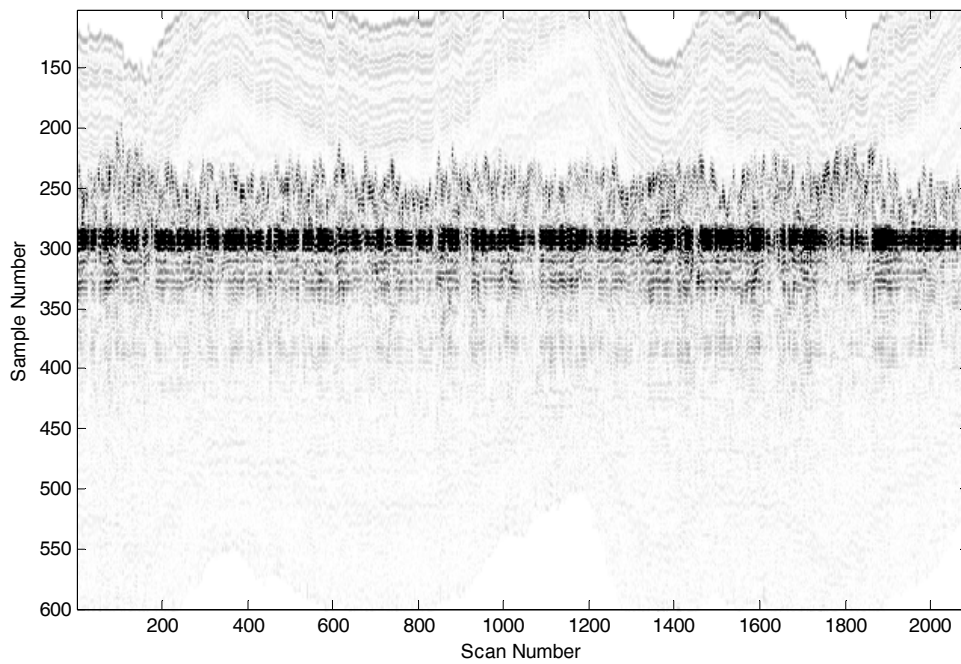


Figure A.3 Aligned profile #574 with a 4 scan running average applied

28
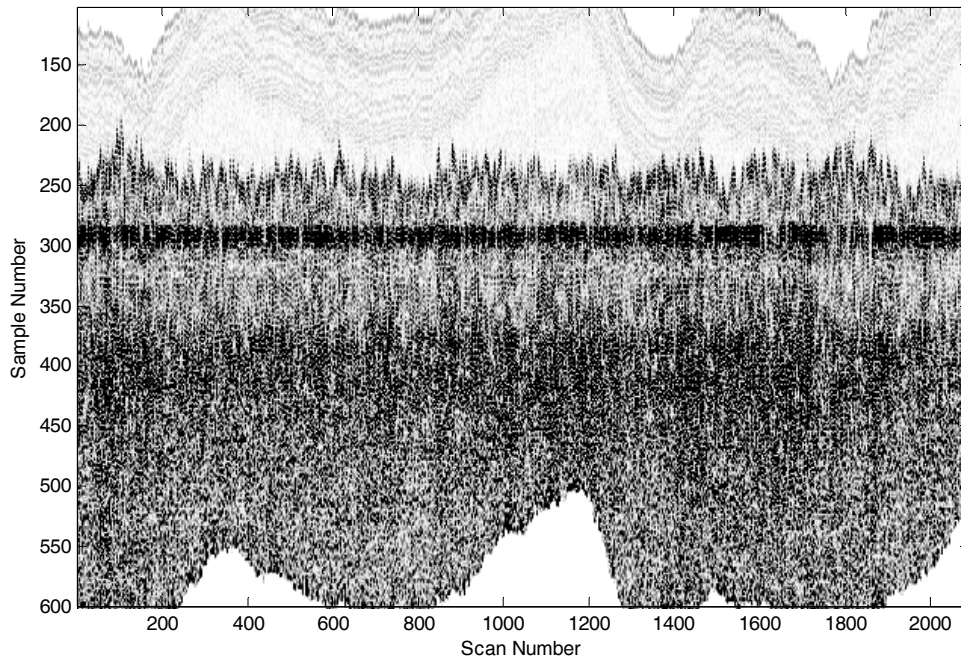
Figure A.4 Aligned profile #574 with a time varying gain applied
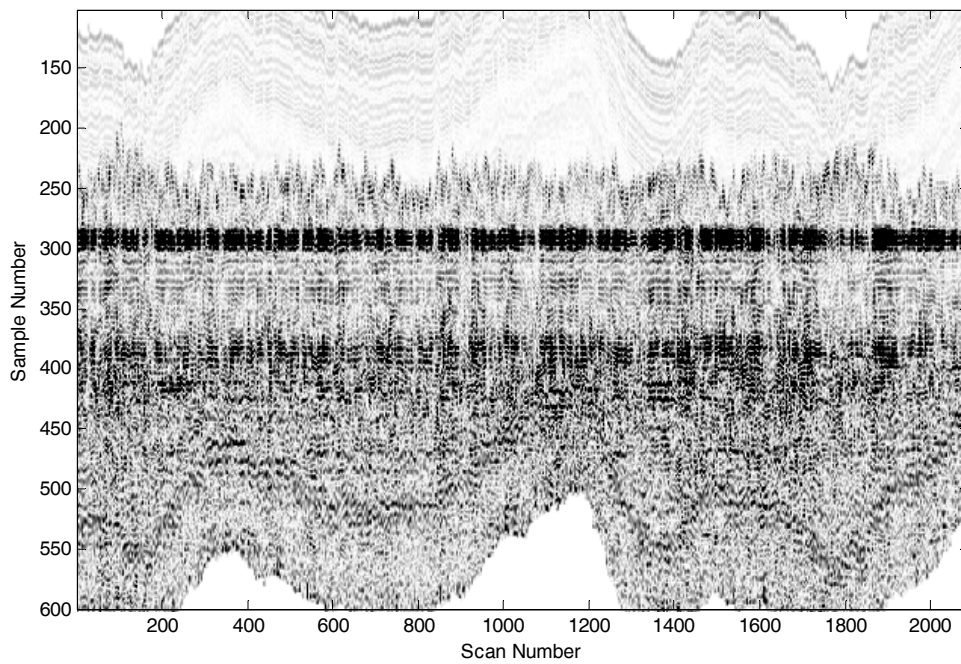


Figure A.5 Aligned + time gain profile #574 with a 4 scan running average applied
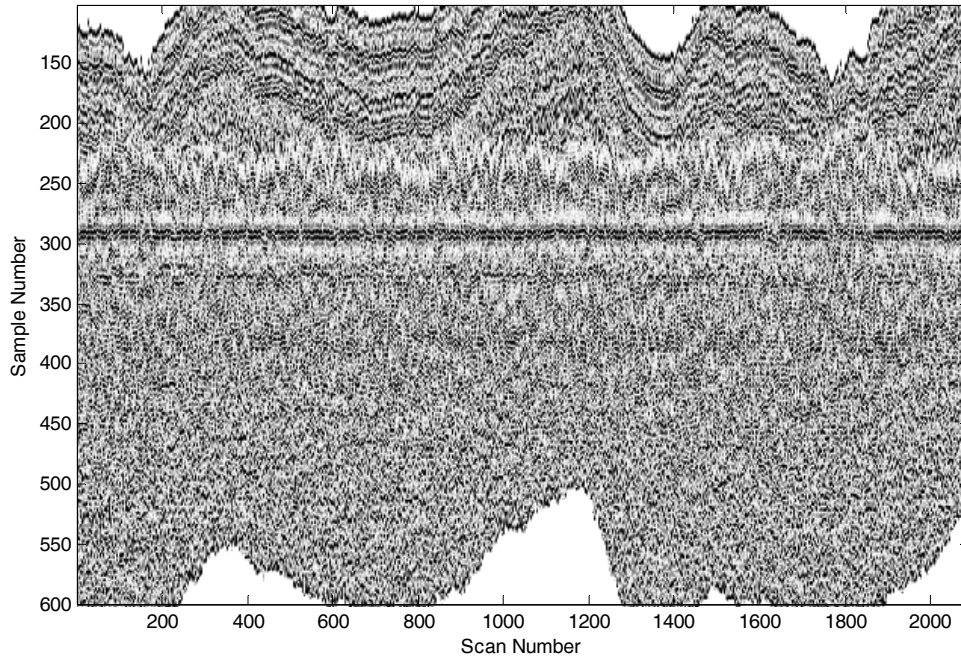
Figure A.6 Aligned profile #574 with automatic gain control applied
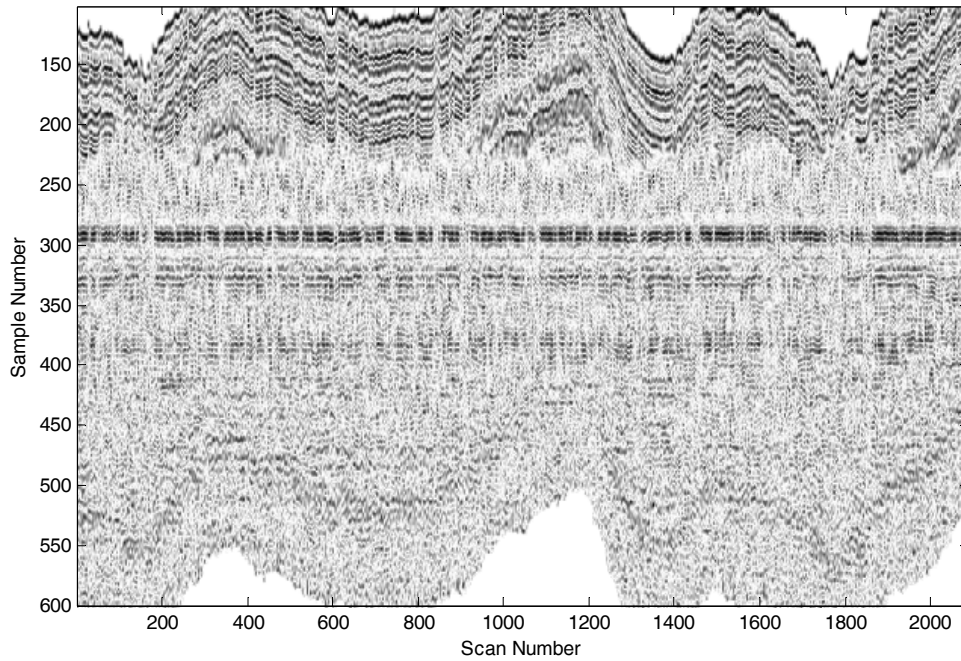


Figure A.7 Aligned + AGC profile #574 with a 4 scan running average applied

Site 2 – GPR Profile #575

As with Profile #574 shown in Figure A.1, Figure A.8 shows the profile for Site 2 #575 with the same processing and smoothing of the bottom of snow arrival time.
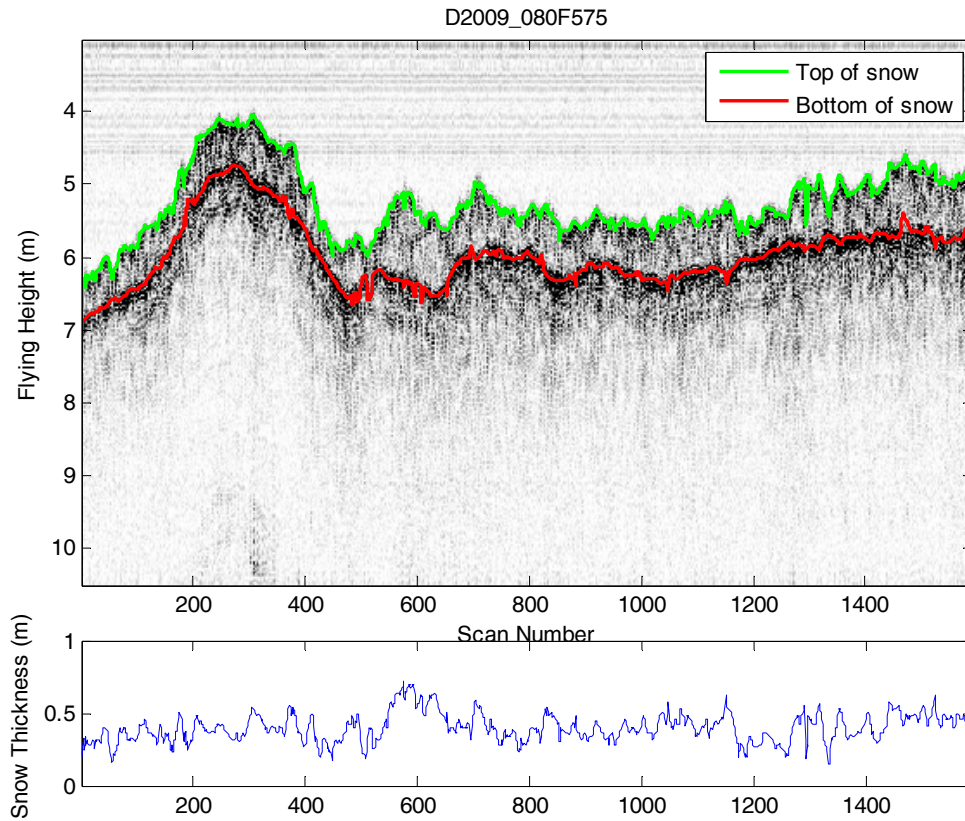


Figure A.8 Site 2 GPR Profile #575 data plot and snow thickness result

- Figure A.9 - Use the location of the top of the ice to align the GPR data so that the ice echo appears as a straight line across the plot
- Figure A.10 - Apply the running average to data with time-varying gain applied
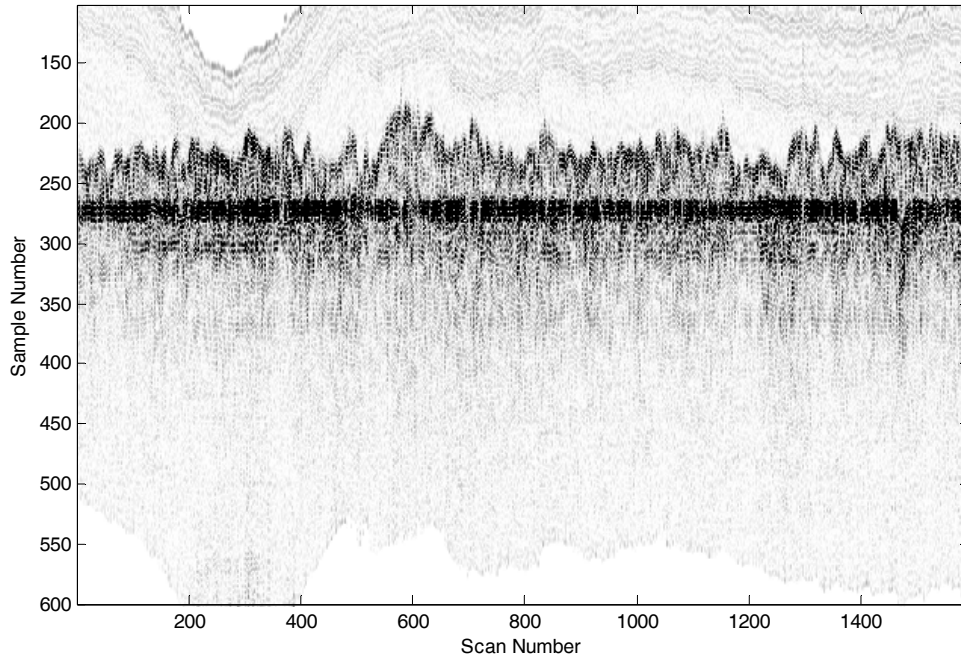
Figure A.9 GPR Profile #575 aligned to flattened out the ice echo
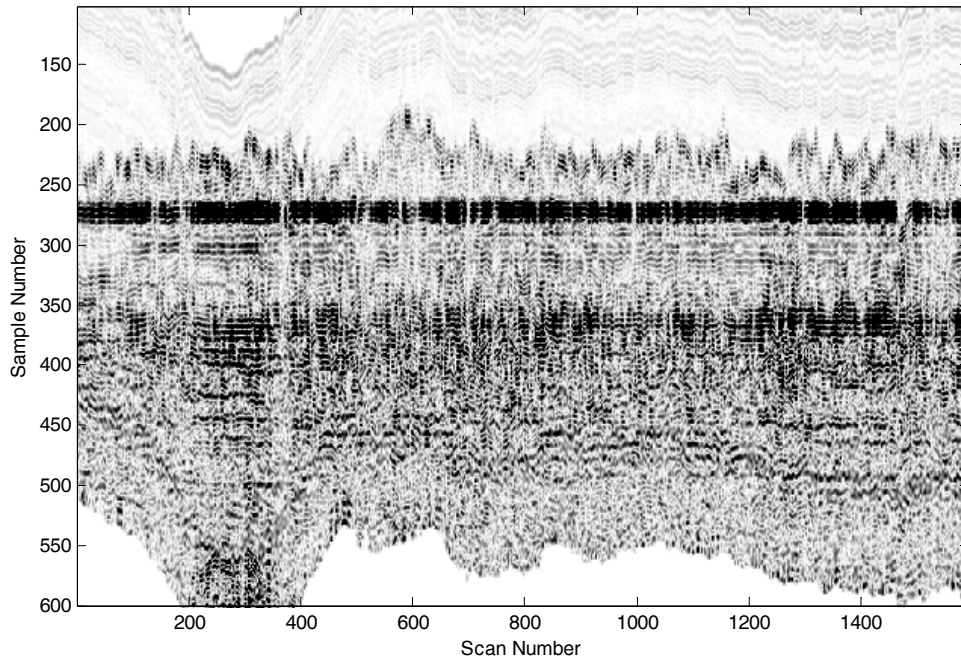


Figure A.10

Site 3 – GPR Profile #579

The Site 3 profiles (numbers 579 and 580) are more difficult to work with as the sample outlier removal routine used for the Site 2 profiles could not handle the rapid helicopter elevation change in the Site 3 data. As a result, the alignment plot has some large glitches that should be ignored. The snow thickness results for profile #579 are shown in Figure A.11.

Figure A.12 shows profile #579 with the GPR data aligned using the bottom of snow (top of ice) echo location from the snow thickness processing. Figure A.13 shows the GPR profile after applying a time varying gain and applying trace averaging to remove clutter.
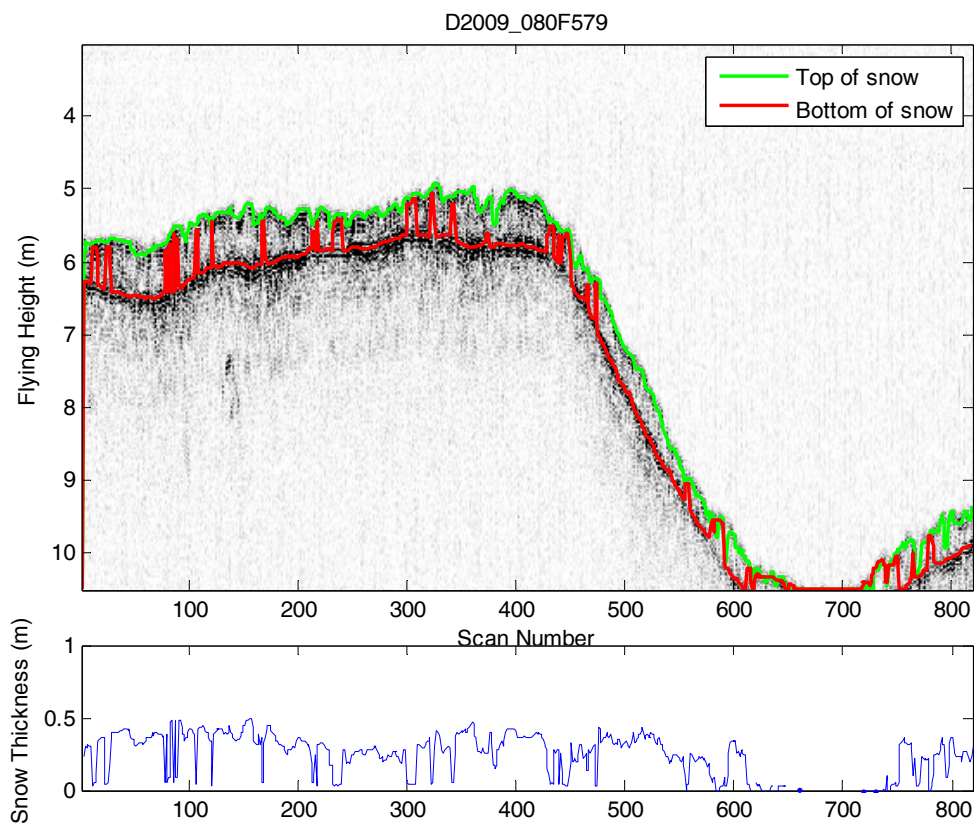


Figure A.11 Site 3 GPR Profile #579 data plot and snow thickness result
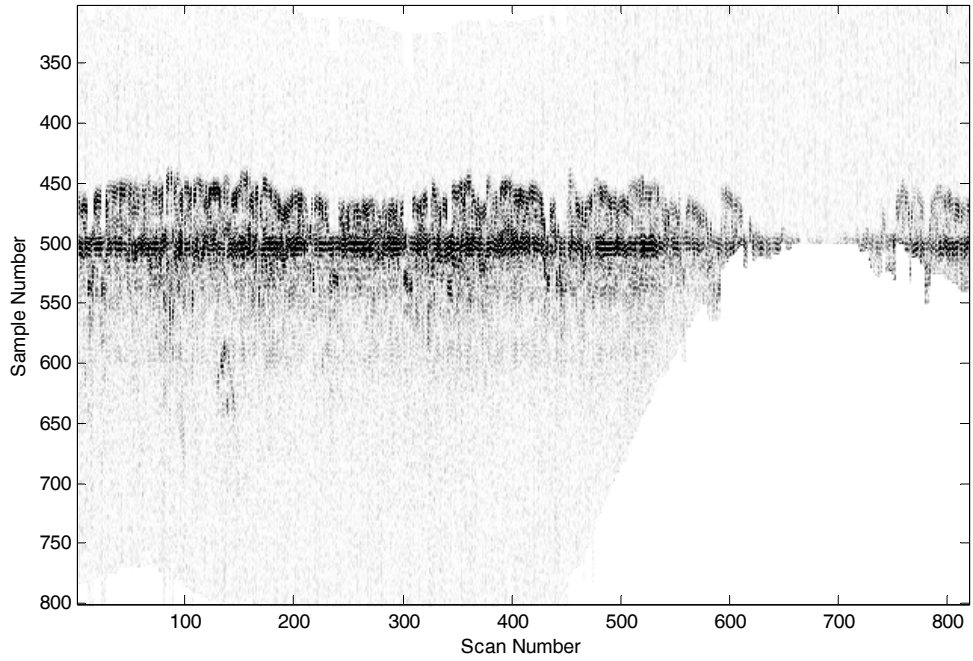
Figure A.12 GPR Profile #579 aligned to flatten out the ice echo
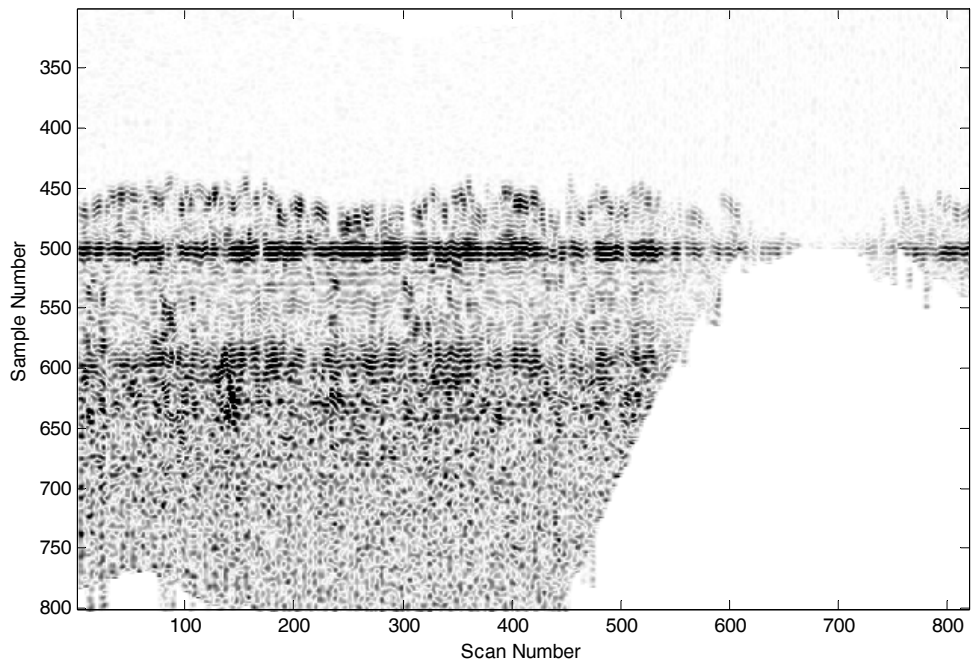


Figure A.13 Aligned + time gain profile #579 with a 4 scan running average applied

Site 3 – GPR Profile #580

The snow thickness results for profile #580 are shown in Figure A.14.

Figure A.15 shows profile #580 with the GPR data aligned using the bottom of snow (top of ice) echo location from the snow thickness processing. Figure A.16 shows the GPR profile after applying a time varying gain and applying trace averaging to remove clutter.
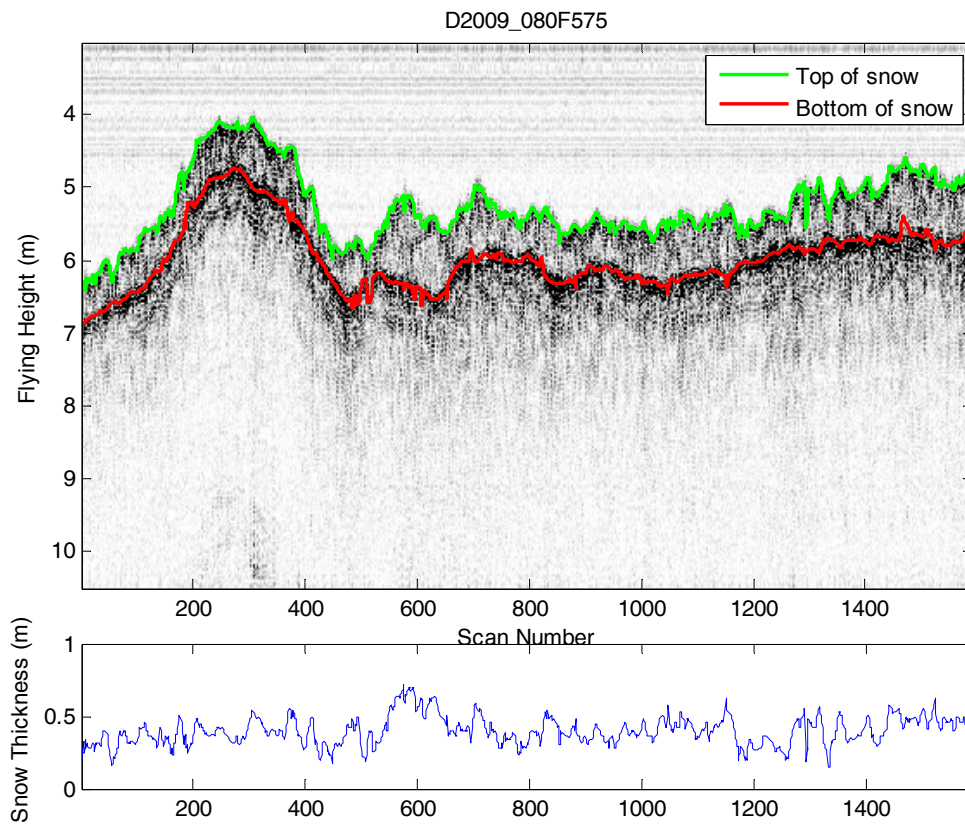


Figure A.14 Site 3 GPR Profile #580 data plot and snow thickness result
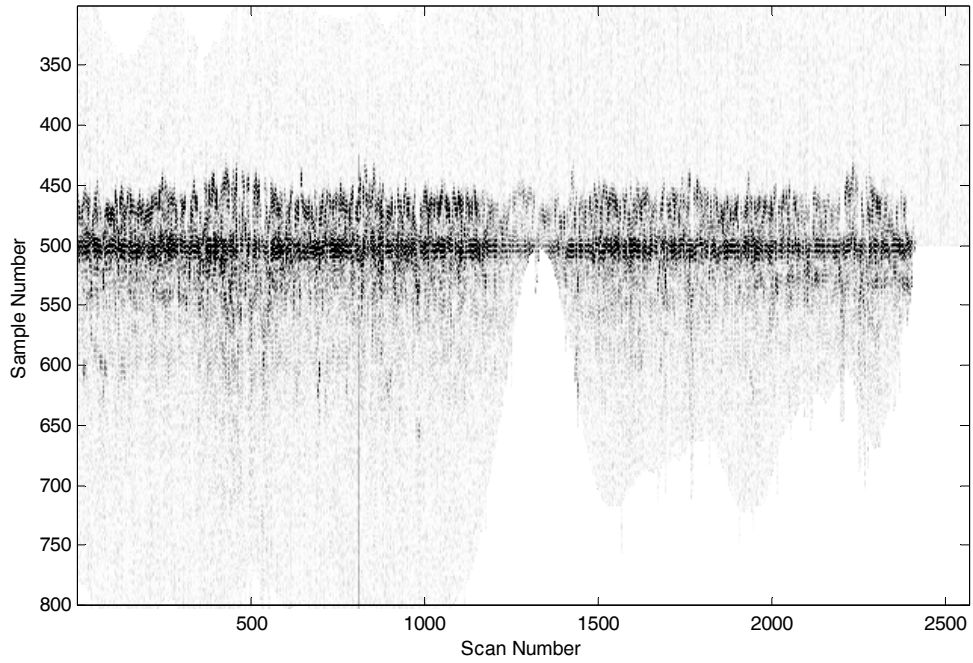
Figure A.15 GPR Profile #580 aligned to flatten out the ice echo
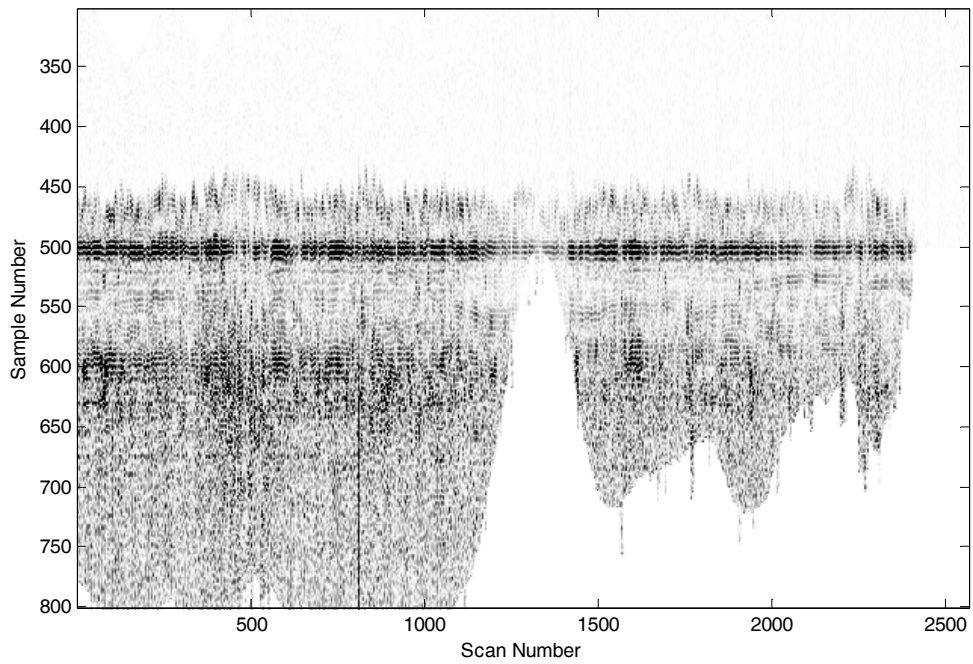


Figure A.16 Aligned + time gain profile #580 with a 4 scan running average applied